FINAL REPORT

FIBER-OPTIC INTERCONNECTION NETWORKS FOR SPACECRAFT

For the Period May 22, 1990 through May 21, 1992

Prepared for

NASA

Goddard Space Flight Center

Attn.: Mr. John Rende

Greenbelt, MD 20771

In Performance of

CONTRACT No. NAS5-30896

May 1992

OPTIVISION, INC.

4009 Miranda Ave., Palo Alto, CA 94304 (415) 855-0200 Fax: (415) 855-0222

Table of Contents

Table of Figures and Tables

1. Introduction

1.1 Summary

This document is the final report for the Phase II SBIR entitled "Fiber Optic Interconnection Networks for Spacecraft," contract number NAS5-30896. This work was performed during the period from 22 May 1990 to 21 May 1992 for the NASA Goddard Space Flight Center under the technical direction of John Rende, Code 735. The principal investigators were Dr. Antonio R. Dias for the first year and Dr. Robert S. Powers for the second year of the contract. Primary technical contributors were Kelvin Chau, Dan Knapp and Steve Gutierrez for switch design, fabrication and test, Dr. Larry R. McAdams for radiation testing, and Drs. Alexander A. Sawchuk and Joseph W. Goodman for system architecture and application.

The overall goal of this effort was to perform the detailed design, development and construction of a prototype 8x8 all-optical fiber-optic crossbar switch using low-power liquid crystal shutters capable of operation in a network with suitable fiber-optic transmitters and receivers at a data rate of 1 Gb/s. During the earlier Phase I feasibility study [1], it was determined that all-optical crossbar system has significant advantages compared to electronic crossbars in terms of power consumption, weight, size, and reliability. This result is primarily due to the fact that no optical transmitters and receivers are required for electro-optic conversion within the crossbar switch itself.

A verbatim listing of the Phase II statement of work is as follows:

- Optivision, Inc. will design, fabricate and deliver one 8x8 fiber-optic crossbar switch, operating at 1300 nm, with single mode input fibers and (50 μm core) multimode output fibers. The shutter technology to be used in this system is TBD; it will be either FLC or PDLC. The switch will have an insertion loss under 25 dB (lower if PDLC shutters are used). Its reconfiguration time will be on the order of 10 ms. The switch will be able to switch data at rates exceeding 1 Gb/s at 10^{-9} BER. To accomplish this objective, the following tasks will be undertaken:

  Task 1 - Preliminary Design

  Task 2 - Initial Test

  Task 3 - Final Design

  Task 4 - Fabrication and Final Tests

  Task 5 - Ongoing Analysis

- Optivision will integrate this crossbar system in the CHRPS project (as outlined in Task 7).
- Optivision will work closely with NASA's procurement office toward acquisition of suitable fiber-optic transmitter/receiver systems suitable for insertion in this system.
- Optivision will work closely with the NASA contractors involved in the development of the Input-Output Buffer Formatter (IOBF) for appropriate integration in the CHRPS project.

All tasks described above were successfully completed during the Phase II effort. An 8x8 matrix vector multiplier (MVM) architecture optical crossbar switch was constructed. Polymer dispersed liquid crystal (PDLC) shutters were selected over ferroelectric liquid crystal (FLC) or lead lanthanate titanate zirconate (PLZT) shutters because of their low power requirements, simple drive electronics, lack of polarization sensitivity, and small insertion loss.

The switch delivered on this contract had significantly improved performance compared to previous optical crossbar switches in terms of reduced size, reduced power consumption, lower insertion loss, and improved loss uniformity. An average insertion loss of 14.8 dB was obtained, with a total variation of 2.3 dB across all combinations of input and output ports. The average optical extinction ratio for the switch was 18.5 dB, while typical shutter turn-on and turn-off times were 10 and 30-40 msec, respectively, suitable for the particular NASA application.

The 8x8 crossbar switch was delivered in December 1991 and fully integrated into the CHRPS Test Bed in January 1992, in sufficient time for use within the CHRPS demonstration conducted on 28 February 1992. The PCO transmitters used in the CHRPS Test Bed have a nominal output power of 0 dBm, while the corresponding PCO receivers have a sensitivity of -27 dBm. Thus, the delivered switch, with an average 14.8 dB insertion loss, has a residual link margin of 12.2 dB.

Figure 1-1 shows a front view of the crossbar switch. Figure 1-2 shows a top-front view of the switch with the front and top panels removed. The two 32 element PDLC arrays are evident on the right side of the photo, along with the electrical connections and the fiber-optic couplings units interfaced to the arrays. The total volume of the delivered switch was 1.34 cu. ft. Weight for the prototype was less than 30 pounds. Power consumption was 34 watts. Size, weight and power would be substantially reduced in a space-qualified optical switch. Figures 1-3 and 1-4 are a photograph and a block diagram, respectively, of the CHRPS Initial Test Bed configuration which incorporated the Optivision crossbar switch.

Figure 1-1. Front view of Optivision 8x8 crossbar switch.

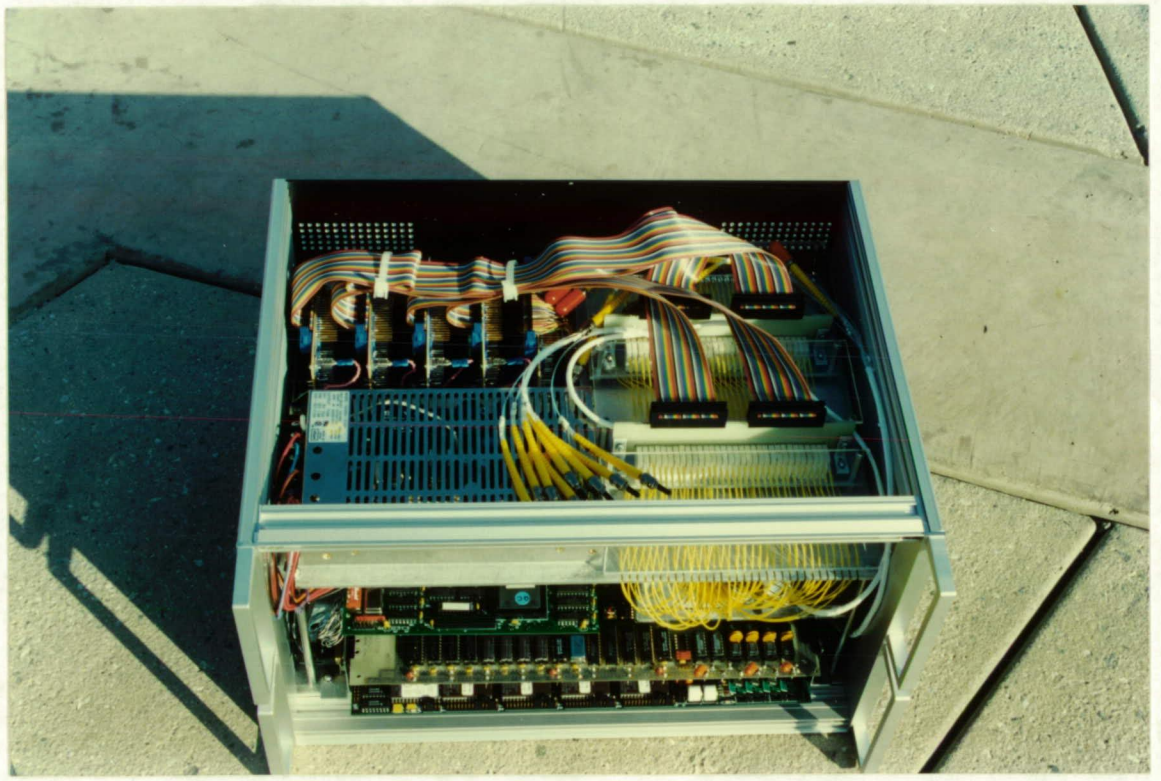

Figure 1-2. Top-front view of crossbar switch, with front and top panels removed.

Figure 1-3. Photograph of CHRPS initial Test Bed configuration.

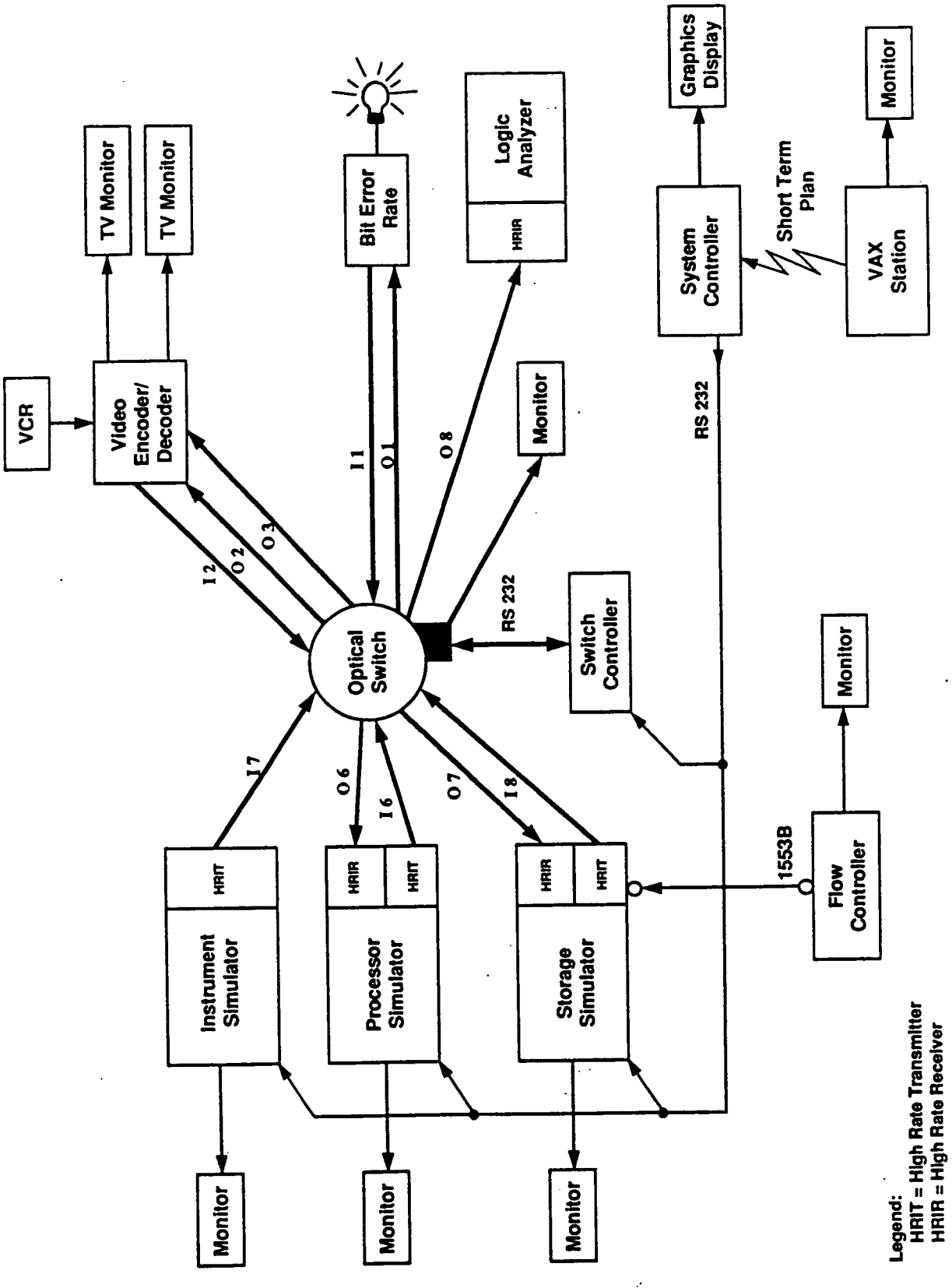

Figure 1-4. Block diagram of CHRPS Initial Test Bed configuration.

During the course of the development of the deliverable crossbar switch on this contract, an existing PDLC-based crossbar switch was upgraded (with funding provided by a related contract) and loaned to NASA/GSFC. This loaner was useful from the perspective of NASA gaining early knowledge of the operation of an optical crossbar switch and facilitating the integration of the final switch into the CHRPS Test Bed. In addition, Optivision acquired, tested and delivered to NASA/GSFC, under related contract funding, five 678 Mb/s PCO transmitter/receiver pairs, one 800 Mb/s Gazelle HOT ROD coax interface card, and four sets (3 dB, 10 dB, 15 dB, and 20 dB) of Gould attenuators, all of which were integrated into the CHRPS Test Bed.

Section 1.1 of this report has summarized the technical goals, objectives and accomplishments of the Phase II SBIR effort. Section 1.2 gives background information on the need for optical switching in a spacecraft environment and summarizes work accomplished during the Phase I SBIR effort. Section 2 describes the optical, electrical and mechanical (packaging) design of the crossbar switch. Section 3 contains performance measurements of the individual switch components and the overall switch and compares these performance measures to the component allocations and system requirements. Section 4 discusses the major issues, experiments performed and the measurement results pertaining to the irradiation testing of key components of the optical switch. Section 5 contains conclusions and recommendations for the effort required to bridge the gap between the proof-of-principle switch technology demonstrated here and the technology required for a space-qualifiable switch. Section 6 contains references. The report concludes with the required NASA Form 1626, Report Documentation Page.

1.2 Background

This section summarizes the need for high speed optical switching in future spacecraft interconnection networks and briefly describes how the Optivision crossbar switch system fits into the Configurable High Rate Processing System (CHRPS) demonstration. This section also discusses requirements for optical switches in a space environment, briefly reviews optical vs. electronic switching, and summarizes conclusions of our Phase I effort.

1.2.1 High Speed Networks for Spacecraft

The development of advanced spacecraft systems over the next decade (1992-2002) requires the use of very high speed on-board data networks to support various communications and signal processing systems. Fiber optics offers significant potential advantages in this environment because of its well-known high bandwidth capabilities (exceeding 1 Gb/s), reduced interference, EMI and RFI, and power, weight, and size advantages. The on-board data communication requirements of future systems such as the polar orbiting platform (POP) and the Space Station

will require interconnection networks that operate over fiber-optic lines with space-division switches.

Toward this goal, NASA Goddard has been working on various fiber-optic network test bed systems to demonstrate the feasibility of the concept before final systems are designed for flight testing and insertion in a flight-qualified system. These systems are called CHRPS (Configurable High Rate Processing System). Various CHRPS Test Bed systems operate at data rates ranging from 125 Mb/s to rates in excess of 1 Gb/s. The major components of CHRPS are a fiber-optic crossbar switch located at a central hub (for circuit switched communications), a set of fiber-optic transmitters and receivers, and fiber-optic links and interfaces to electronic instruments, processors, mass storage devices, controllers and communications links.

In Phase I of this program, Optivision examined alternative technologies and specific components to implement the fiber-optic crossbar switch in an advanced CHRPS network Test Bed, and developed a specific design for a high performance fiber-optic crossbar [1]. The important issues in the design are the physical constraints of power, reliability, weight, size, radiation hardness and other environmental factors, and that the crossbar must eventually be flight-qualifiable for use in space.

1.2.2 Configurable High Rate Processing System (CHRPS) Architecture

A block diagram of the CHRPS ground-based Initial Test Bed was shown in Fig. 1-4. The overall configuration includes several instruments, processor and storage simulators connected to an 8x8 (eventually 16x16) fiber-optic crossbar switch at a central hub. All heavy lines in the figure are fiber-optic lines. The crossbar must be capable of full nonblocking broadcast or multicast operation (i.e. any single input or any set of inputs is each capable of sending data to multiple outputs or to all outputs). A system controller sends commands to the various devices and the crossbar to set up and remove connections These control signals are sent by RS 232 serial lines to the devices. The interfaces in each device perform data input, output and formatting. Various types of integrated fiber-optic transmitters and receivers can be used to convert the electronic signals to and from the optical domain. Data encoding (such as 4B/5B or 8B/10B) is needed in the transmitters, receivers, and interfaces to simplify clock recovery and synchronization in the physical fiber-optic link.

A system with a similar architecture will be used in flight hardware. For spacecraft applications, the components must be low in power, weight and size and must be reliable and space-qualifiable. Another major consideration is the radiation hardness requirements imposed by the planned polar

orbits of future spacecraft. The radiation requirements and some experimental measurements of optical crossbar switch components are summarized in Section 4 of this report.

In Phase I of this program, we defined and compared two basic techniques for implementing the fiber-optic crossbar network in terms of power, weight, size, reliability and radiation hardness. One approach uses an all-optical passive crossbar, while the other uses electronic active crossbar switches. In addition, fiber-optic transmitters and receivers which are part of the network were considered.

1.2.3 All-Optical Crossbar Implementation

Figure 1-5 shows one alternative implementation for the on-platform CHRPS system using an all-optical fiber-optic passive crossbar switch. The crossbar switch here is a passive device that acts as a light pipe whose internal connection paths are set electronically by the crossbar controller, which in turn receives instructions from the system controller. If there are N devices to be interconnected by the network, then a total of N fiber-optic transmitters and receivers is needed.

1.2.4 Electronic Crossbar Implementation

An alternate design using an electronic crossbar switch was considered early in Phase I of the program and is illustrated in Fig. 1-6. This design is similar to the all-optical design shown in Fig. 1-5, except that an electronic crossbar switch replaces the optical crossbar switch shown. In addition, N extra transmitters and N extra receivers are needed at the outputs and inputs, respectively, of the electronic crossbar. In this implementation, signals from the electronic interfaces to the various instruments, processors and other devices are converted to optical form as in the previous implementation, but then must be converted back to electronic form by an additional receiver for each line at the crossbar for electronic switching. After the electronic crossbar performs the signal routing, another transmitter at each line converts the signal back to electronic form to provide the return connection. The major difference from the previous system is that a total of $2N$ fiber-optic receivers and transmitters are needed.

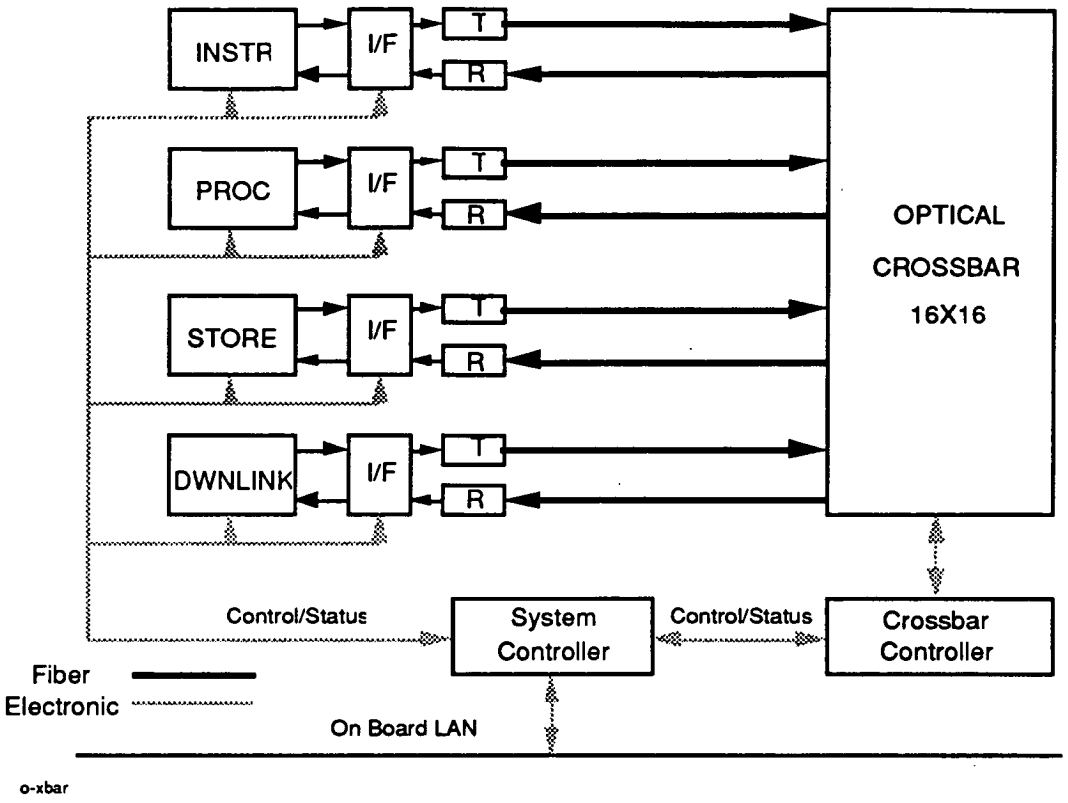

Figure 1-5. Generic on-platform optical crossbar implementation.

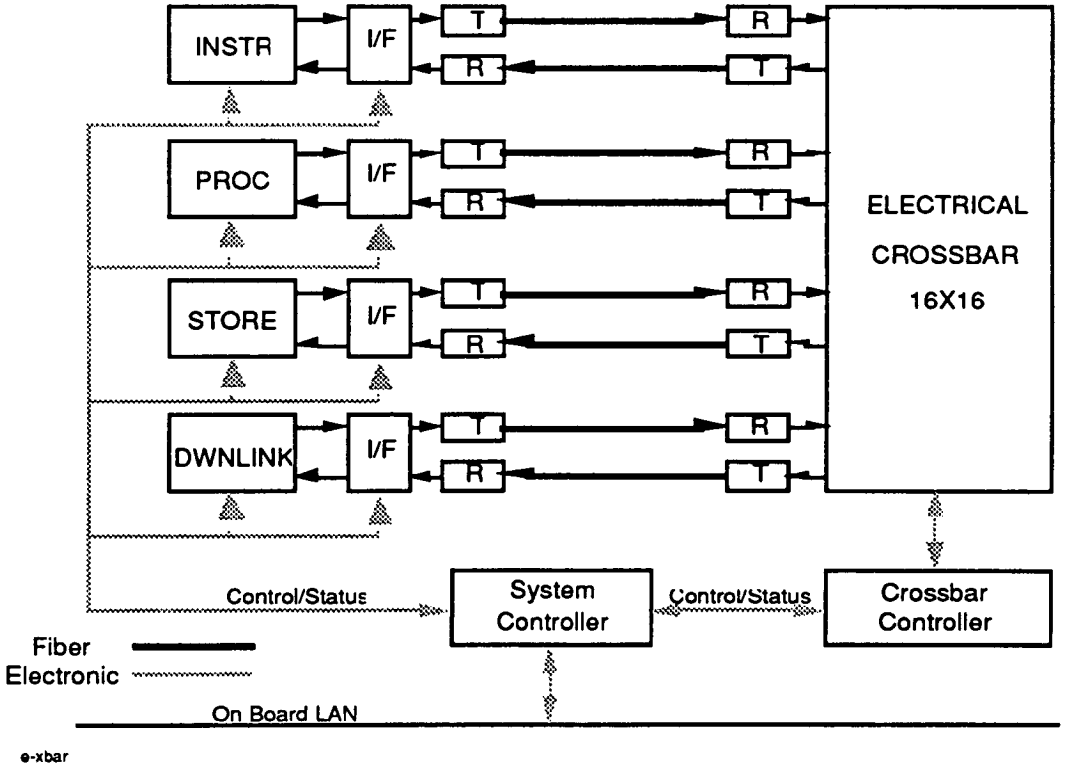

Figure 1-6. Generic on-platform electrical crossbar implementation.

1.2.5 Comparison of Switch Designs and Summary of Phase I Results

After comparing all-optical and electronic technologies for implementing a 16x16 crossbar switch in a space-qualified CHRPS data network, we found in our Phase I study [1] that all-optical crossbar systems have significant savings in power consumption, total weight and total size (savings averaging over 30%) over the electronic equivalent. These savings occur because there are one-half the number of optical transmitters and receivers in the all-optical system: it does not require optical-electronic-optical data conversion at the crossbar switch itself. In addition, the reliability of the all-optical system should be twice as good because there are one-half the number of laser diode sources needed in the optical transmitters. Laser diodes are undoubtedly the most unreliable component in any high speed fiber-optic network design. The Phase I effort made a preliminary study of the radiation requirements imposed on system electronics, optical fibers and optical materials and devices by a polar orbiting platform (POP). The electronics in the controller, drivers, transmitters and receivers can be constructed of high-speed GaAs components, which are inherently radiation hard. The Phase I effort also described several types of single-mode and multimode optical fibers that are suitable for use in space. Many possible improvements in the optical crossbar design were identified, including:

(1) the use of liquid crystal (LC) devices for additional power, weight and size savings,

(2) improved construction to further reduce optical loss,

(3) the use of integrated shutter drive electronics, and

(4) integrated optoelectronic transmitters and receivers at the CHRPS devices.

Some of these improvements have been implemented in the Phase II design and deliverable crossbar switch described in subsequent sections of this report. We also discuss detailed experiments on the radiation hardness of the liquid crystal materials and components used in the switch.

2. Switch Design

This section describes the optical, electrical and mechanical design of the optical crossbar switch developed under this effort. This switch represents a significant advance in mechanical packaging compared to previous switches, providing reduced volume, enhanced reliability and reduced power consumption.

2.1 Optical Design

The design of the NASA/GSFC optical crossbar switch is based on the matrix vector multiplier (MVM) architecture [2] illustrated in Figure 2-1. The system is all-optical and all-passive, in the sense that light injected at an input fiber is coupled to one or more output fibers. No electro-optic conversion is required at the inputs and outputs to the shutter. This architecture is capable of bandwidths greater than 1 Gb/s, with the potential for additional bandwidth with wavelength division multiplexing. In addition, it is compatible with both analog and digital data, and is compatible with many electro-optic shutter technologies. We focused within this program on *passive* shutters which provide no gain to the optical signal.

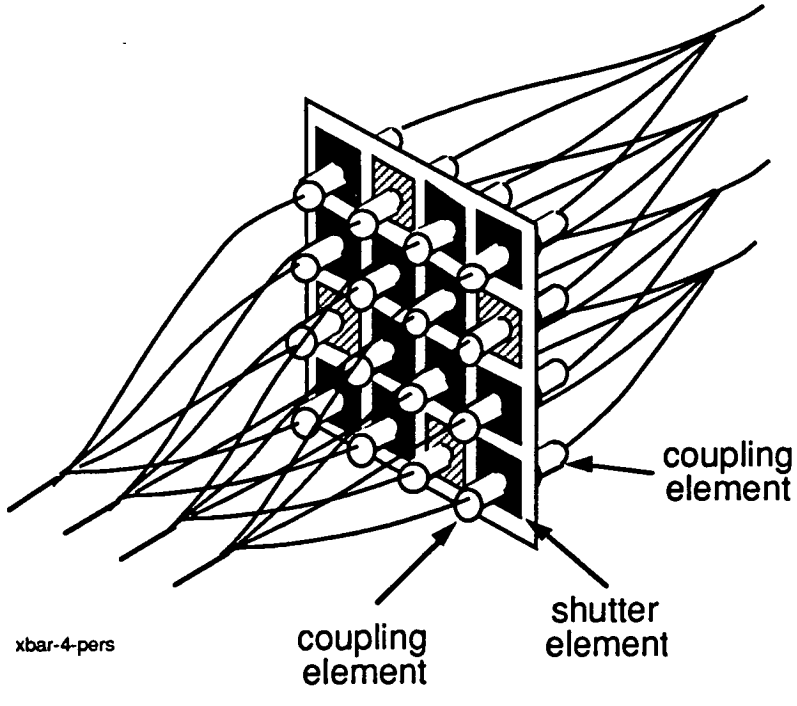

Figure 2-1. All-optical matrix-vector-multiplier (MVM) design.

Each of N incoming fiber lines is split into N separate lines (Figure 2-1 illustrates the case of N=4, while the crossbar actually constructed had N=8). These lines address a vertical column of an NxN

array of electrically activated optical shutters. Collimating lenses (gradient-index lenses) couple the light efficiently through the shutters and into the outgoing fiber. The fibers leaving the shutter array are combined across rows using Nx1 fiber combiners to produce the N outgoing lines. The shutters can be arbitrarily opened or closed; thus the overall interconnection pattern can be a one-to-one permutation of inputs to outputs, a *broadcast* of any input to the remaining outputs, or a *multicast* of several inputs to the remaining outputs. It is also possible to send several inputs simultaneously to the same output (*wire-oring*).

A trade-off study was performed at the beginning of the effort to determine the most appropriate shutter material for use in an optical switch destined for a space environment. The electro-optic shutters used in previous Optivision 4x4 and 16x16 optical crossbar switches were made of the electro-optic ceramic PLZT (lead lanthanate zirconate titanate). PLZT exhibits a variable birefringence depending on the electric field applied perpendicular to the direction of light propagation (a Kerr cell). The PLZT shutters effectively rotate the polarization of incoming light under electrical control, so that light emerging from the shutter undergoes a variable degree of attenuation depending on the orientation of an output polarizer.

Liquid crystals are long chain molecules having birefringent properties somewhat similar to that of PLZT. In operation, the LC material is oriented in a cell (usually two parallel plates made of glass, polymer, or other optically transparent material). Metallic or transparent electrodes are attached and the assembly is placed between polarizers. The degree of birefringence is controlled by an external electric field; thus the device can act as an electronically-controlled shutter.

By varying the orientation and chemical composition of the LC material, many unusual properties are available. One type of LC material is ferroelectric (FLC material), and has molecules with two stable states of birefringence. FLCs can be used to make a shutter having two stable states (memory) which can altered by application of a switching field. In operation, the FLC cell is placed between crossed polarizers exactly as with PLZT shutters, and an external electric field toggles the cell between the two states. All LC devices have the advantages of very low operating voltages and power requirements; however, they switch in a time somewhat slower than PLZT (generally on the order of 100 μs). For typical FLC devices (a very large aperture (1 cm) shutter), the switching voltage is on the order of 20 v.

Another variation on the use of LC materials is a new process called polymer-dispersed liquid crystals (PDLC). No polarizers are used with these devices; thus they are potentially much more light efficient than FLC devices. Figure 2-2 shows the principle of operation of PDLC devices. The birefringent LC molecules are embedded in a polymer binder in a random orientation within a

cell having transparent electrodes. With no applied voltage across the cell, incoming light rays see LC molecules whose indices of refraction are very different from the polymer binder; thus the rays are highly scattered and very little energy passes directly though. When a voltage is applied (typically 20 - 30 v), the LC molecules orient themselves to line up with the applied field, and the index seen in this orientation is set to be the same as that of the polymer binder, so that the cell passes almost all (> 90%) of the light. The turn-on time of these devices is typically 10 ms, while the turn-off time is 10s of ms, depending on the applied voltage.

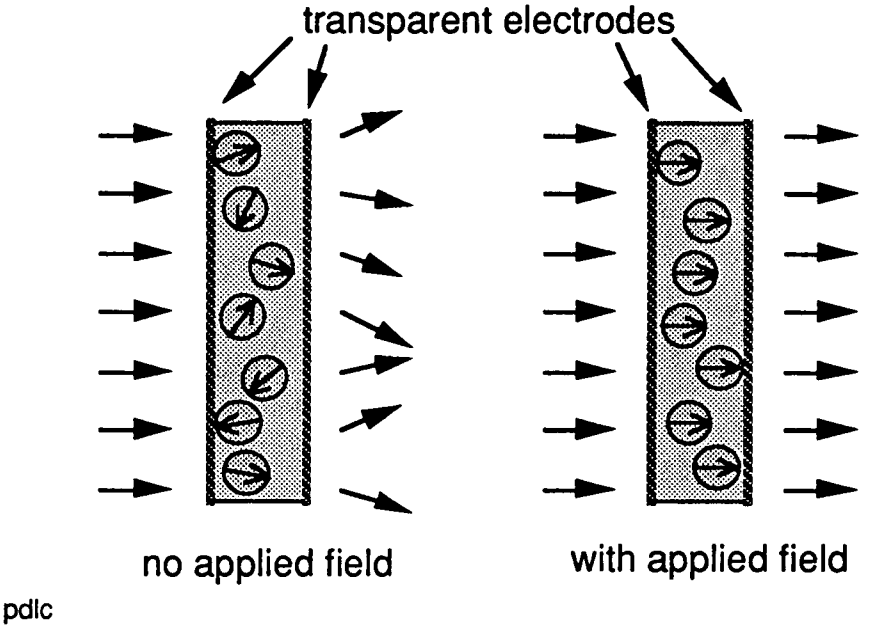

Figure 2-2. Polymer dispersed liquid crystal (PDLC) switching mechanism.

These low power devices require much lower voltages and simpler drive electronics. PDLC devices are attractive because they rely on electrically switchable scattering and use no polarizers. In addition, they are highly transparent. For these reasons, PDLC was selected as the shutter material for use within the NASA/GSFC crossbar switch. The PDLC shutters used in the switch were made by Taliq Corporation in the form on two 32 element arrays. Thus, the topology actually used was a linear topology shown in Figure 2-3.

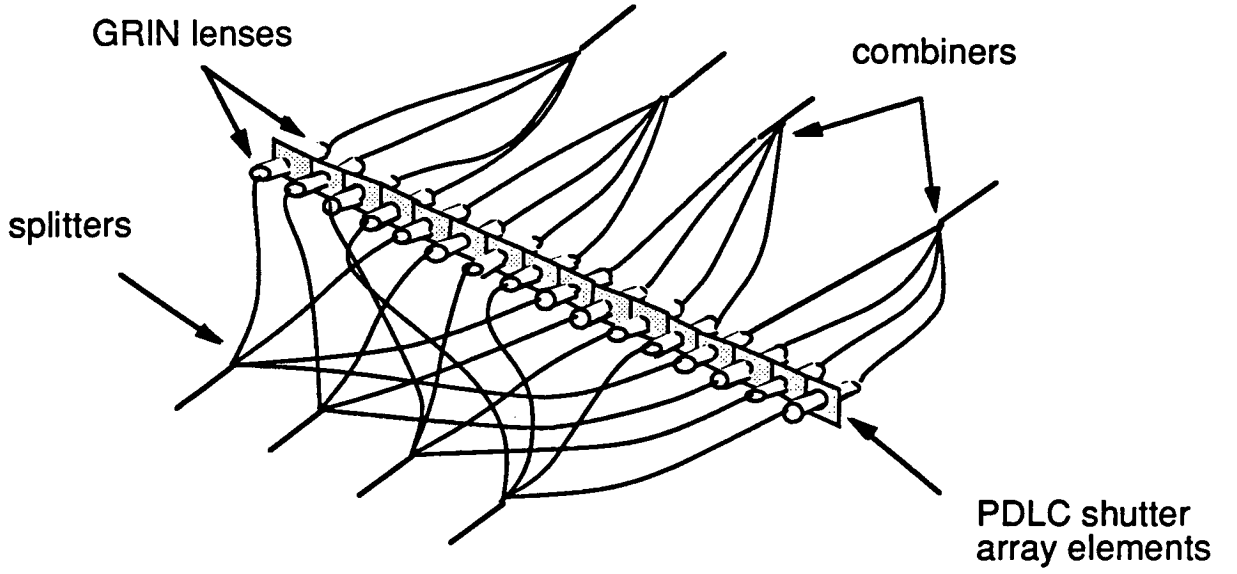

Figure 2-3. Linear topology used for crossbar interconnect. The figure shows 4x1 splitters and combiners and 16 element PDLC arrays. The actual crossbar switch constructed utilized 8x1 splitters and combiners and 32 element PDLC arrays.

2.2 Electronic Design

The crossbar control is performed electronically by individually setting the shutter status of all elements of the switching matrix. To make the control as flexible as possible, a fully parallel addressing design is used; one or all of the shutters can be switched independently and simultaneously.

We briefly review here the design of the control electronics for previous Optivision crossbar switches to lay the foundation for understanding of the controller design approach used for this program. The 4x4 and 16x16 crossbars previously built by Optivision utilizing polarization-sensitive PLZT shutters were required to be reconfigured completely in under 10 μs. For this reason, high speed driver electronics were constructed to supply the 50 V DC signal needed to drive the PLZT shutters. The electronic controller contained a digital buffer to store the required state of all the shutters, and an analog push-pull driver to supply the 50 V drive signal with a transition time of under 10 μs. A separate PC AT (or compatible) computer with interface card and software (supplied by Optivision) was used to control these crossbars. The interface card contains a buffer-sequencer which supplies parallel output signals (16 data bits and 4 address bits) which are sent to the crossbar controller, which was housed in the same chassis as the optics module itself.

The control electronics utilized in the NASA Goddard crossbar switch to drive PDLC shutters is a modification of the circuit technology developed for the PLZT shutters. However, the same basic technology and approach are used. An add-on AC generating signal was designed to accommodate the AC-type signal required by the PDLC shutters. In addition, instead of a separate chassis housing the PC/AT and *interface card*, these components were placed within the same chassis as the *controller cards* and *optics module* in order to provide a more compact unit.

The function of the controller cards is to store and set the functional status of the crossbar switch, namely define the ON/OFF status of each of the 64 shutter elements. There are four controller cards mounted on a motherboard PC-card, in a card cage, near the back left of the crossbar case. Each controller card controls 16 shutter elements and has a piggy-back card to generate the AC waveform required by the PDLC shutters.

The controller electronics input is delivered through a parallel port from the control computer interface card. This port contains 16-data lines, 4-address lines, and miscellaneous control and handshake lines. A single "out" command from the PC/AT sets the status of 16 shutters simultaneously. The address lines identify the controller card associated with a particular crossbar rows of interest. Arbitrarily, the controller cards are organized along crossbar rows, but could just as well be organized along crossbar columns. The latter might be preferable, if broadcast is used often, since the setting of a particular broadcast mode could be accomplished fully in a single clock cycle.

The signals from the control computer interface card are address decoded in the controller motherboard circuitry and routed to the appropriately addressed controller card. The decoding is performed by a 74365 control chip and a 16-bit PAL. Each controller card contains a buffer that stores the status of the current configuration, followed by an analog high voltage driver. A simple piggy-back board circuit is controlled by the logic circuitry and drives the PDLC devices with a signal alternating between -40V and +40V (28V RMS).

The control electronics reconfiguration time is limited by the RC time constant of this AC circuit, which in our present design is rather high, on the order of 100 ms. This value is appropriate in the current application of this system, where reconfiguration time was not at issue. Where there is a need for a faster reconfiguration time, the AC generating circuit can be redesigned to match PDLC's 5 ms switching time.

The physical implementation of this 64-element controller required special care given the need to operate at high speed with low electronic crosstalk. This design performs flawlessly, exhibiting no crosstalk problems which plagued earlier designs. This required extra care in routing of control

and current lines, and in providing appropriate grounding and shielding planes. The motherboard PC is made of 4 layers, and each STD controller card is a 6-layer card.

2.3 Mechanical Design

Figure 2-4 illustrates the overall switch packaging, identifying optics and electronics compartments and locations of major electronic components. Figures 2-5 and 2-6 show more detailed layouts of the optics compartment packaging and electronics compartment packaging, respectively. A major improvement in packaging design compared to the loaner crossbar was the incorporation of the PC/AT mother board, CPU, video board and interface card within the same chassis as the controller cards and optics components. Previously, for the loaner crossbar, these components were housed in a separate chassis. The exterior dimensions of the delivered switch are 17.283" width, 10.472" height, and 12.776" depth, corresponding to a volume of 1.34 cu. ft.

The crossbar switch and controller are driven from power supplies (5V, +12V, -12V, 48V) mounted on two plates of the crossbar module. All supplies are stock off-the-shelf units. No effort was made during this phase of the program to customize the power source towards the goal of minimizing its volume and weight. Power consumption of the switch was 34 watts.

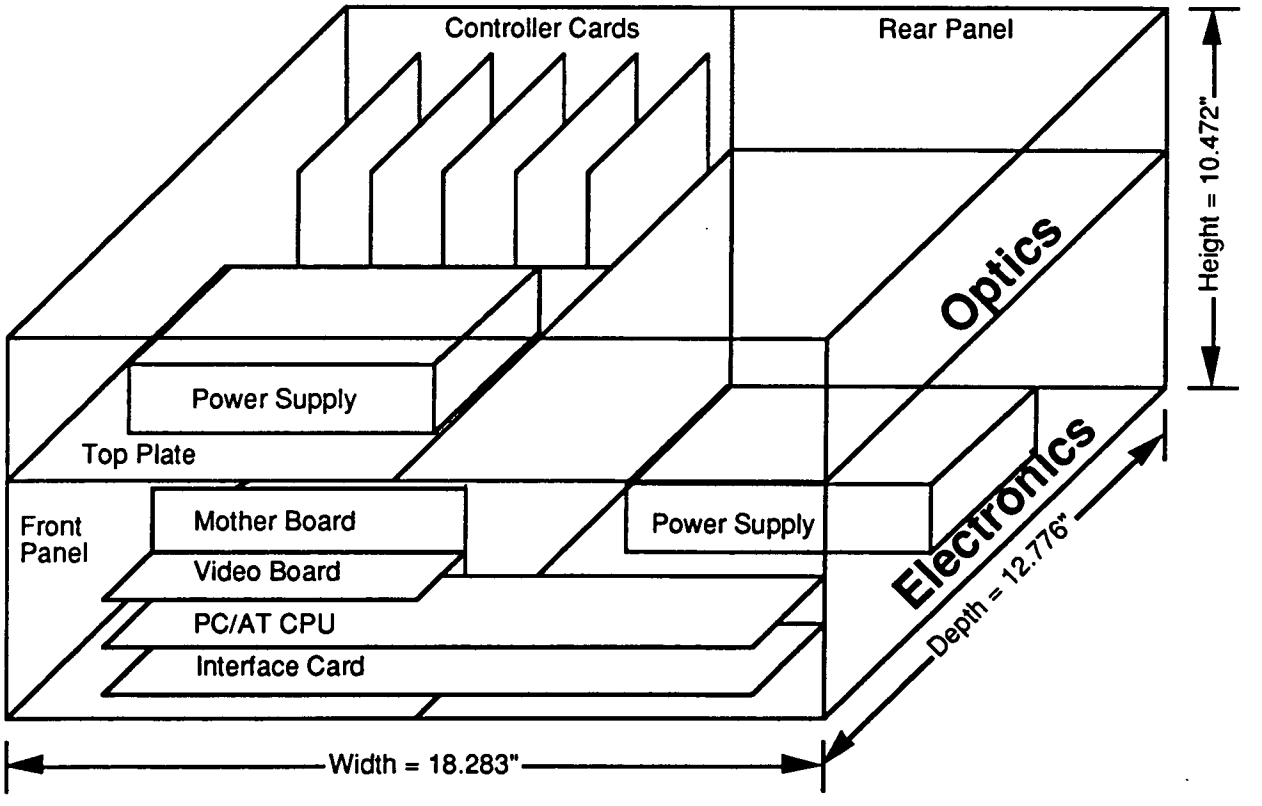

Figure 2-4. Overall switch packaging, showing optics and electronics compartments.

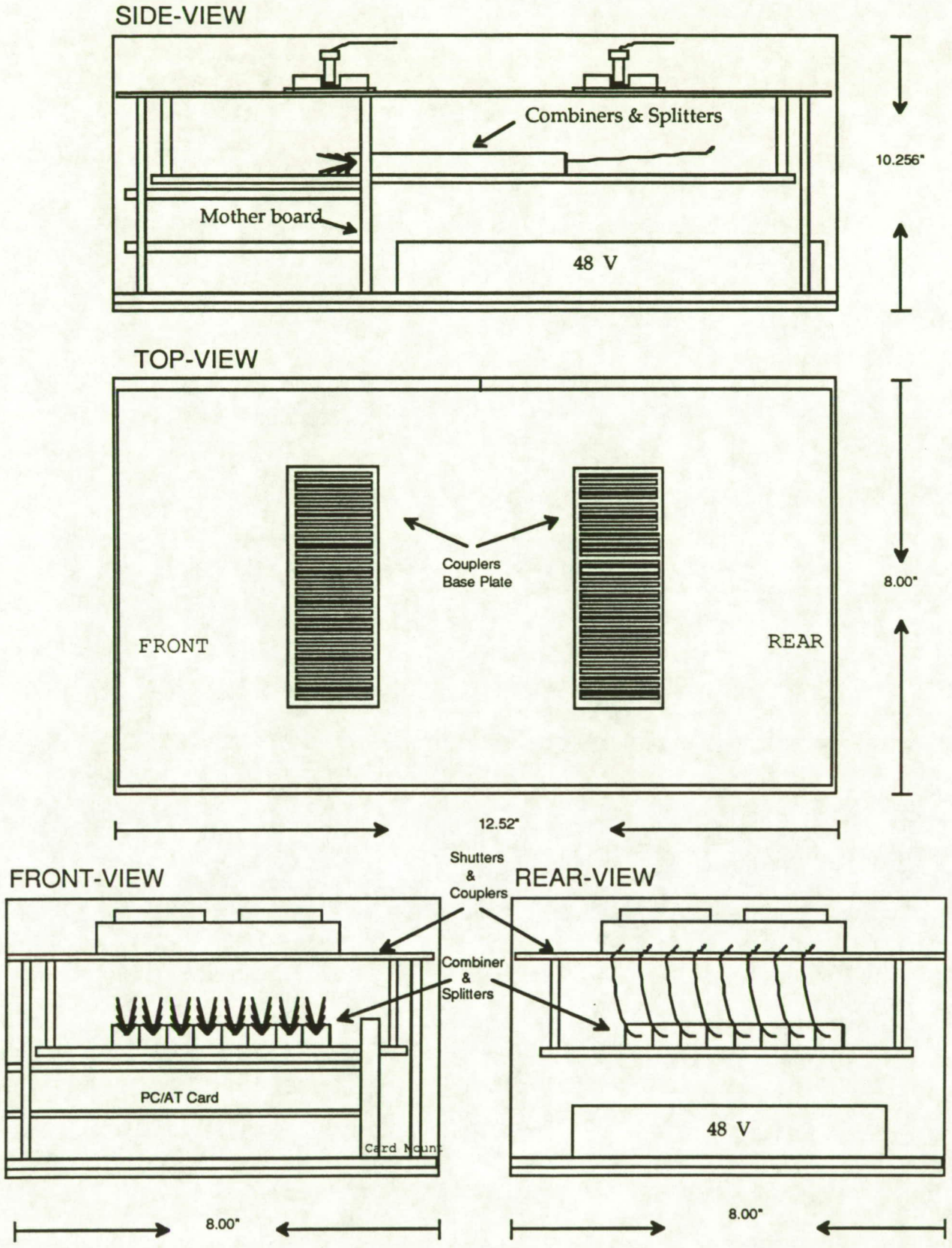

Figure 2-5. Optics compartment packaging.

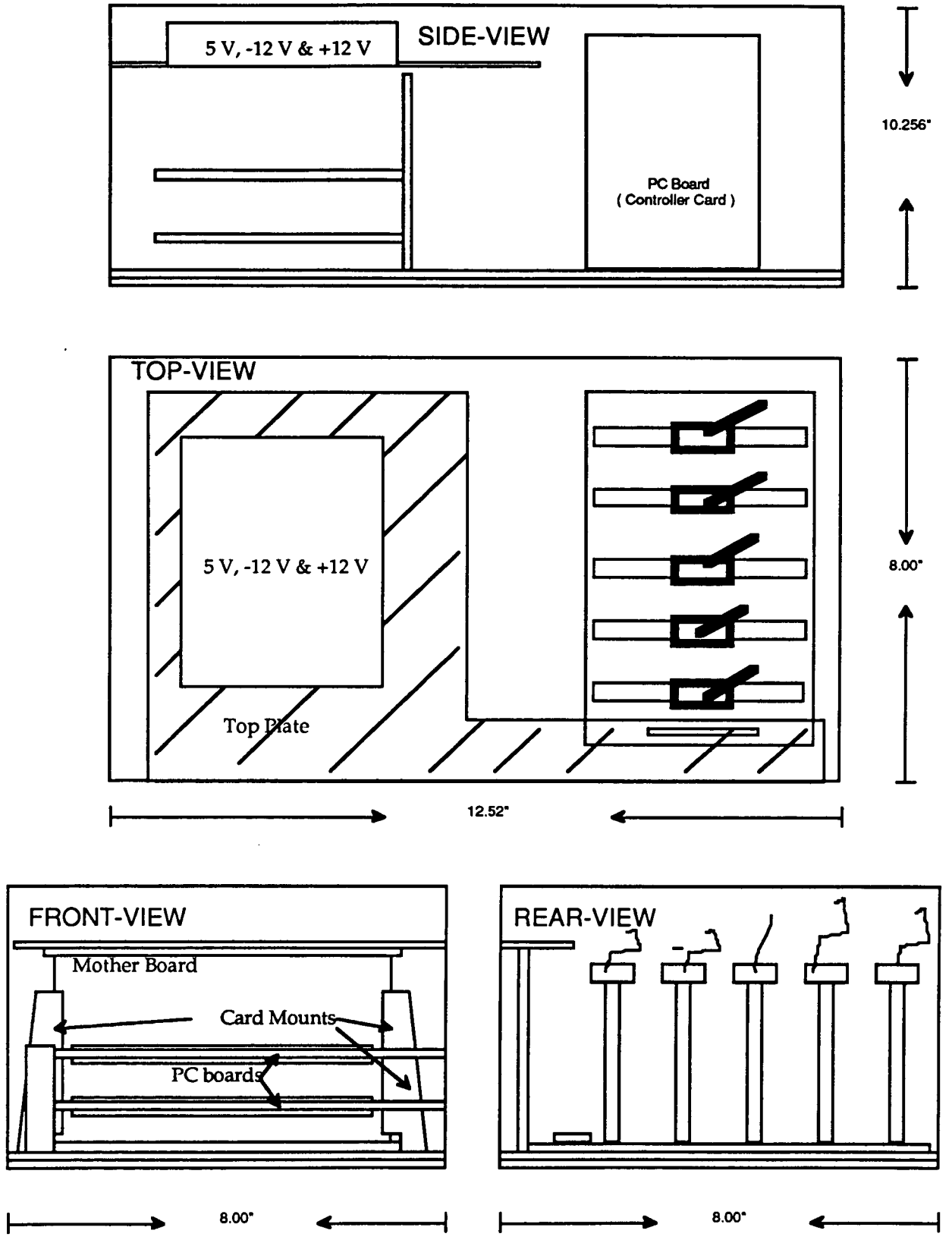

Figure 2-6. Electronics compartment packaging.

3. Switch Performance

This section summarizes the component and overall crossbar system performance values and compares them to the component allocations and system requirements, respectively.

3.1 Power Budget

Figure 3-1 shows the optical power budget. Total system insertion loss based on this allocation to components would be 17.5 dB. Even though the system requirement was for only a 25 dB insertion loss, it was felt early on in the design that significantly improved insertion loss was possible. Note that there is no fan-in loss (except excess fan-in loss) due to the fact that the output fiber is multimode. Considering the 0 dBm transmitter power and -27 dBm receiver sensitivity of the PCO devices to be used in the CHRPS demonstration with this switch, a design link margin of 9.5 dB is available.

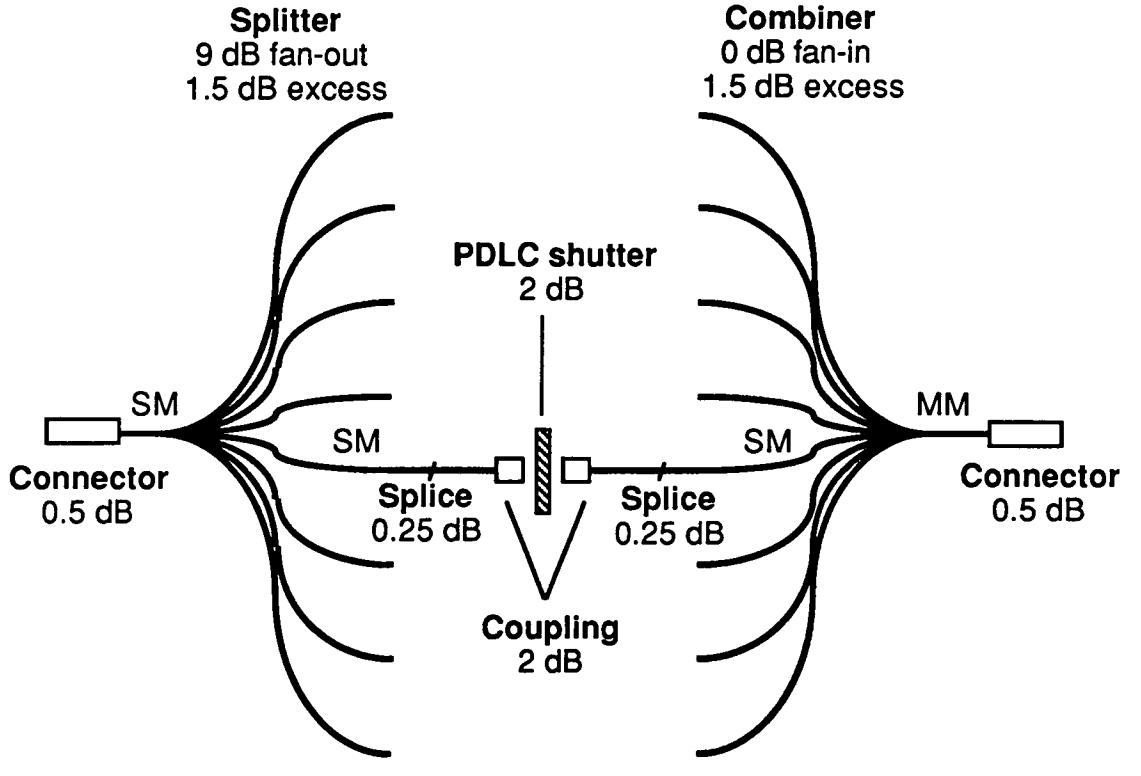

Figure 3-1. Crossbar switch optical power budget.

3.2 Component Measurements

Figure 3-2 summarizes the loss measurements made on the Corning splitters. The average excess loss (above the ideal 9 dB fan-out loss) across all ports and splitters is approximately 1.2 dB. This compares to the 1.5 dB excess splitting loss allocated to the splitters in the optical power budget.

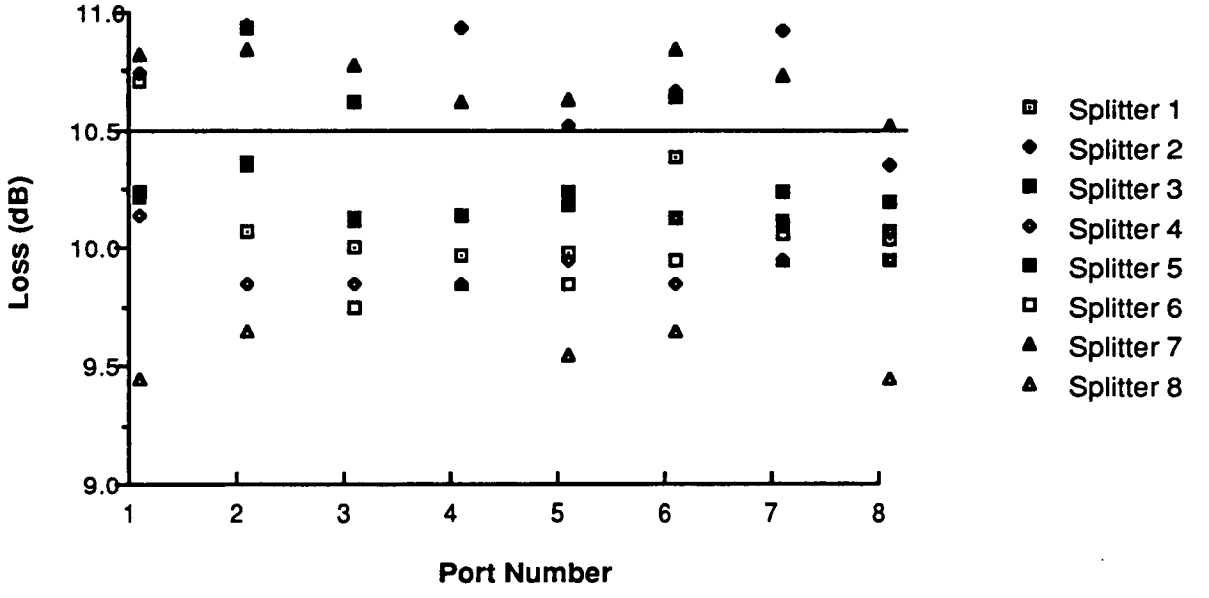

Figure 3-2. Loss map for Corning splitters.

Figure 3-3 shows the loss measurements made on the couplers, which consist of a pair of GRIN lenses for each signal path. The average coupler loss is 1.57 dB compared to the allocated budget of 2.0 dB.

Figure 3-4 summarizes the measurements made on the Kaptron combiners. Three of these combiners (6,7 and 8) were replacements for combiners which did not meet the excess loss specifications. The average excess loss across all ports and combiners is approximately 0.8 dB. This compares to the 1.5 dB excess combining loss allocated to the combiners in the optical power budget.

A balancing process was undertaken to place the splitters, couplers and combiners in a configuration within the crossbar switch such that the loss uniformity across all inputs and outputs was minimized. For example, if a particular splitter output had higher than average insertion loss, a coupler with lower than average insertion loss was used for that particular path.

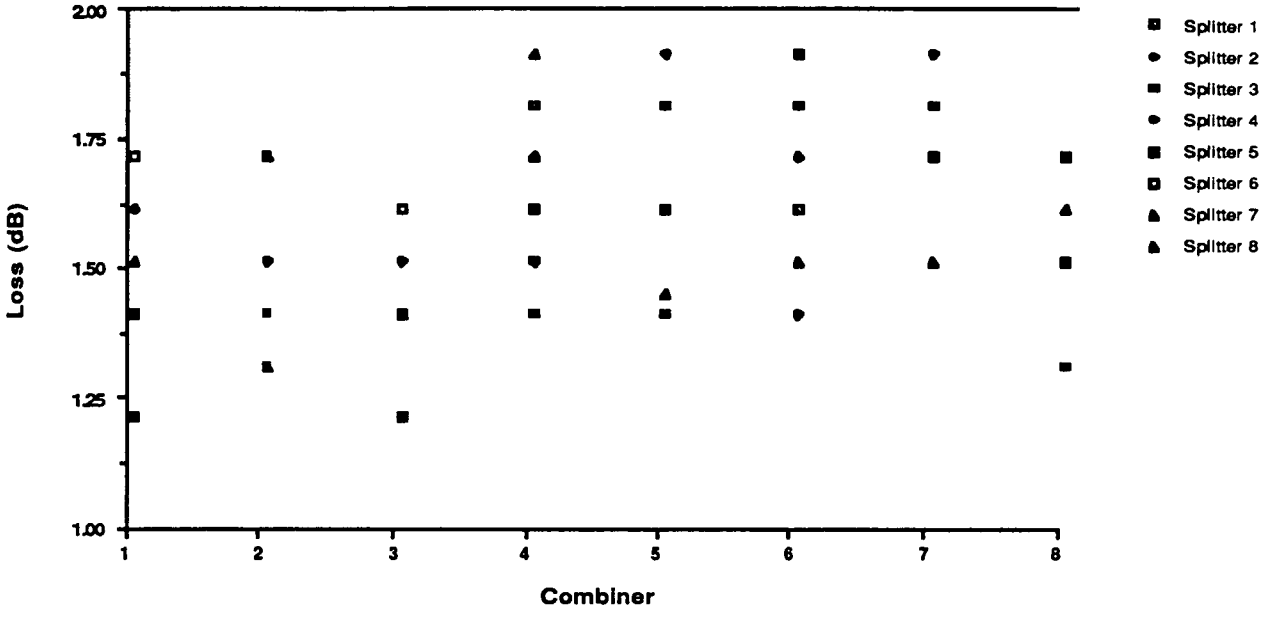

Figure 3-3. Coupler loss map.

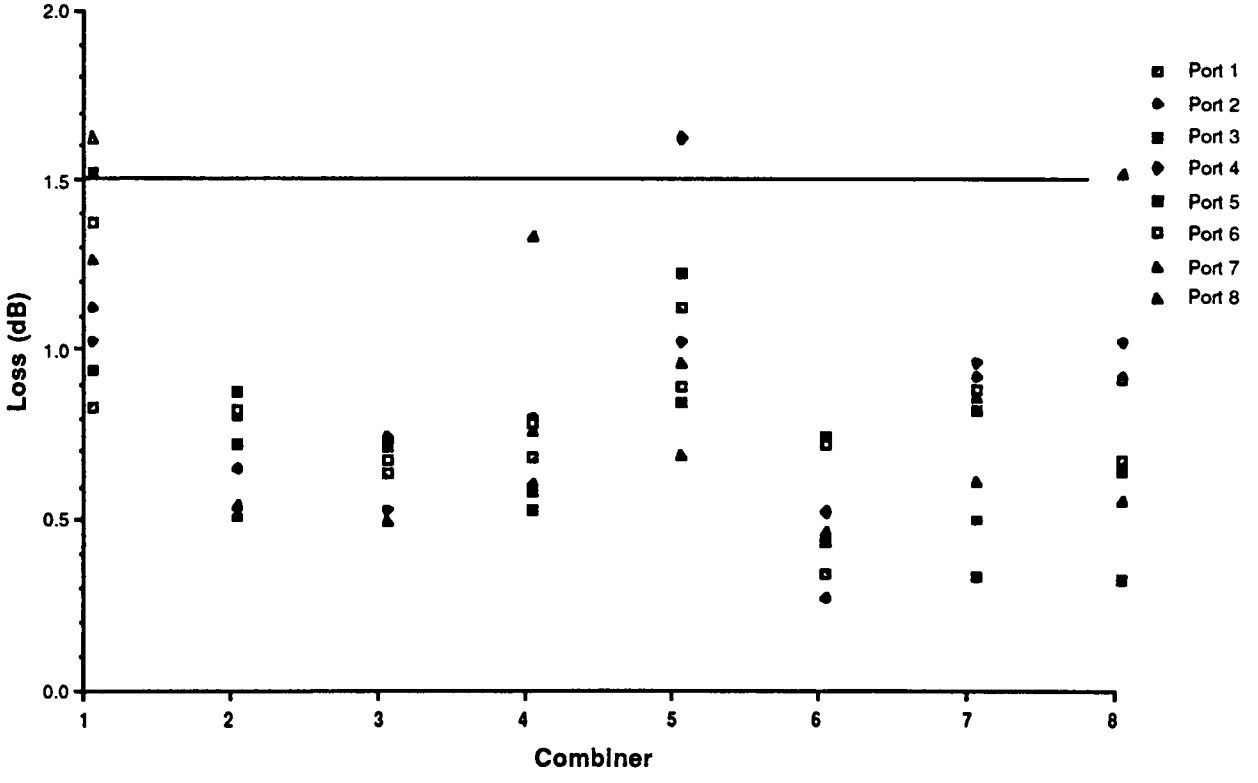

Figure 3-4. Loss map for Kaptron combiners.

3.3 System Measurements

Measurements were made of the optical insertion loss for all possible paths through the switch, as shown in Figure 3-5. Average insertion loss is 14.8 dB, compared to the power budget allocation of 17.5 dB and the contractual requirement of 25 dB, both of which are indicated on the figure. Total variation of insertion loss over all ports is 2.3 dB.

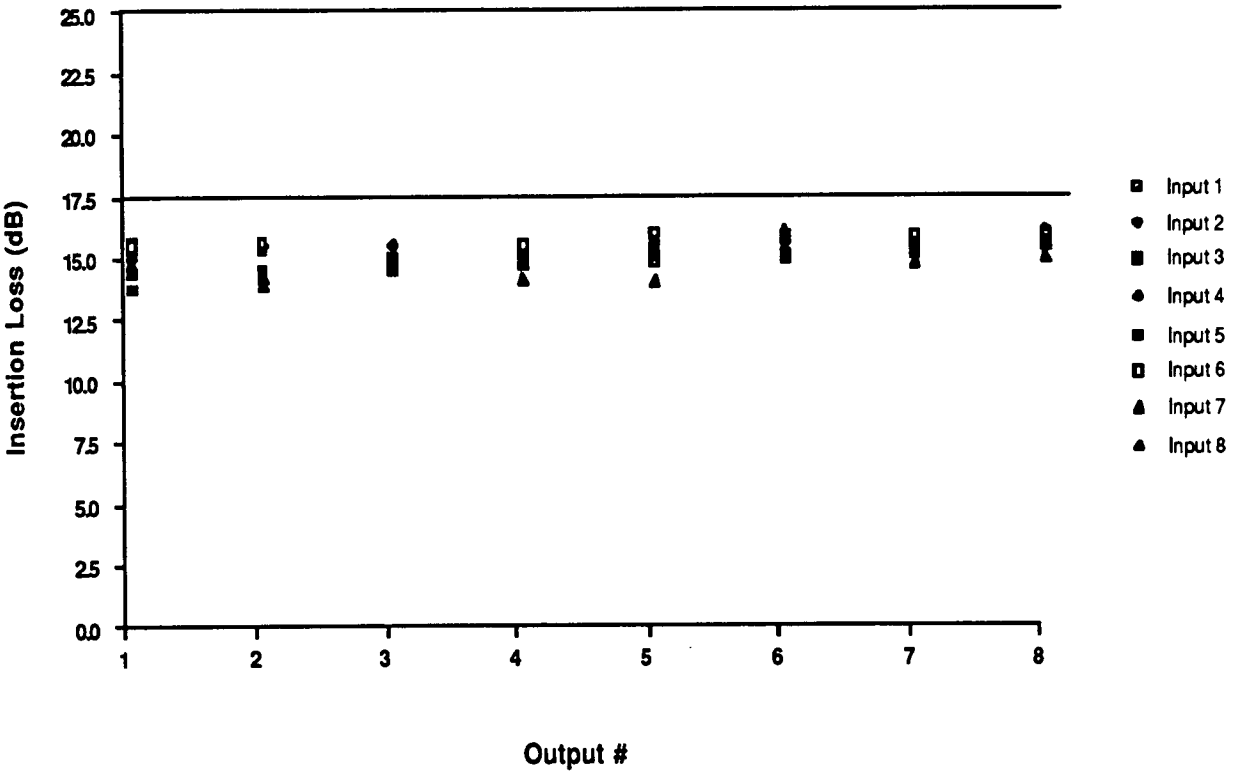

Figure 3-5. Total insertion loss map.

Both the average insertion loss and the insertion loss uniformity represented a significant improvement compared to previous Optivision optical crossbar switches, including the crossbar loaned to NASA/GSFC for familiarization and initial CHRPS interfacing. The loaner switch had an average insertion loss of 17 dB with a total variation of 4 dB. These improvements were due to a combination of improved components (splitters and combiners), improved design (ceramic couplers instead of aluminum couplers), and improved fabrication techniques.

Insertion loss measurements made at different times after assembly of the switch were found to be very consistent, indicating good stability of performance. The measurements shown in Figure 3-5

were made several weeks prior to the visit of Fred Larrick of EER on 10 December 1991 for the purpose of observing switch performance and accepting the switch for delivery to NASA/GSFC. Insertion loss measurements made during that visit gave results which were very similar to those given in Figure 3-5. This consistency of measurements gives an indication of good performance stability for the crossbar.

Extinction ratio measurements made during the Larrick visit of 10 December 1991 are shown in Figure 3-6. The average extinction ratio is 18.5 dB compared to the system requirement of 20 dB.

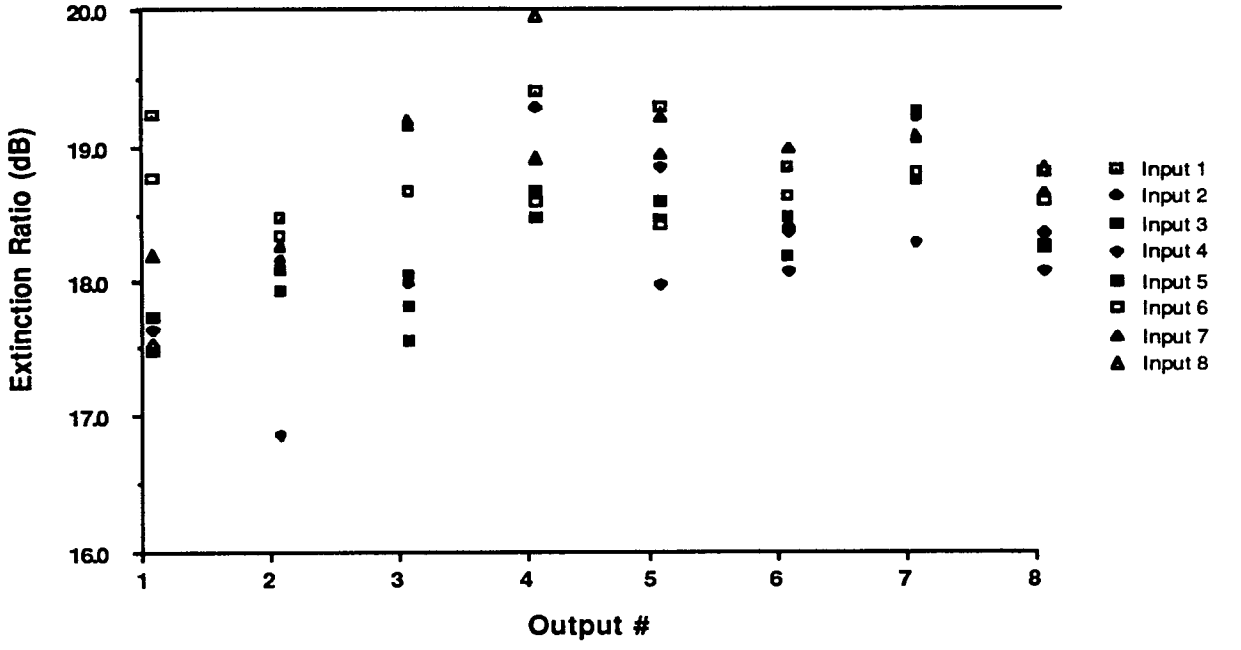

Figure 3-6. Extinction ratio map.

Measurements were also made of the shutter turn-on and turn-off times for the switch. Typical turn-on and turn-off times were 10 and 30-40 msec, respectively, compared to the system reconfiguration time requirement of "on the order of 10 msec." Turn-off times are longer than turn-on times since the birefringent liquid crystal molecules take longer to relax to random orientations when the applied field is removed than they take to align to the field when it is applied.

3.4 Power, Weight, and Physical Size

Contributions to the power consumption for the delivered prototype 8x8 crossbar were as follows:

≈ 14 watts	single board computer (PC/AT) CPU, backplane, and video card
≈ 4 watts	interface cards

< 16 watts	4 controller cards
< 1 watt	PDLC shutters (64 elements = two 32 element arrays)

Total power consumption for the crossbar was ≈ 34 watts. It is worthwhile to note that the power consumption of the PDLC shutter elements is a small percentage of the overall power consumption of the crossbar. As previously noted, the size and weight for the delivered prototype crossbar were 1.34 cu.ft. and < 30 pounds, respectively.

Although the PCO transmitters and receivers utilized in the CHRPS Initial Test Bed are no longer in production, it is instructive to summarize their power, weight and size requirements in order to get an idea of the overall *system* requirements, not just those of the crossbar switch itself. The PCO transmitters and receivers consume 3.5 watts and 0.5 watts each, respectively, at room temperature. Size and weight of each element are estimated at 0.1 cu.ft and 0.5 pounds, respectively. Thus, these components would contribute a total of 32 watts, 1.6 cu.ft. and 8 pounds to an 8x8 crossbar switch system which has 8 transmitters and 8 receivers.

For a space-qualified system, improved packaging and system integration would reduce these requirements dramatically.

4. Radiation Testing

During the course of this program, an obvious question which needed to be answered was the sensitivity of the components used in the proof-of-principle optical crossbar switch system to the expected radiation environment in space for relevant NASA platforms. These components include PDLC shutter arrays, optical fiber, GRIN lenses, splitters, combiners, transmitters, receivers, and electronics. An initial literature search and discussions with experts in the field yielded limited information on some of these components [3-8].

A number of experts in the field of liquid crystals were consulted, including Mark Handschy of Displaytech, Paul Drziac of Taliq, Uzi Efron of Hughes, Frank Allen of E.M. Merck, John West of Kent State, and Carlos Vargas-Aburto of Kent State. The conclusion of these discussions was that there was some concern that radiation might damage PDLC cells due to the presence of organic molecules. Potential radiation effects are darkening, resulting in higher insertion losses, or higher conductivity, requiring higher operating voltages. Some qualitative darkening of PDLC samples irradiated in an accelerator had been noted by Dr. Vargas-Aburto [9]. Since little or no information existed concerning PDLC shutters and GRIN lenses, experiments were designed and carried out to make some preliminary measurements on the radiation sensitivity of these components.

Section 4.1 describes the assumed radiation environment in space which was used to develop the types and levels of radiation used in the experiments. Sections 4.2 and 4.3 summarize known radiation effects on GaAs electronic devices and optical fiber, respectively, based on the literature search. Section 4.4 describes the quantitative electron and proton irradiation experiments carried out by Dr. Carlos Vargas-Aburto of Kent State University at NIST and Western Michigan University, respectively. Insertion loss and extinction ratio measurements for the irradiated PDLC arrays and insertion loss measurement for the irradiated GRIN lenses are presented.

4.1 Assumed Radiation Environment

Several relevant NASA contractor documents were reviewed [10,11] in order to help specify the types and levels of radiation to be used in the experiments. This review is summarized as follows. A polar orbiting platform (e.g. 705 km altitude, 98.2° inclination angle) is subject to high levels of several types of radiation because of its particular (polar) orbit, including:

(1) free electrons (10^4 rads),

(2) Bremsstralung radiation (80 rads),

(3) geometrically trapped protons (2500 rad),

(4) solar flare protons (2500 rads), and

(5) cosmic rays, mostly alpha particles.

Particle energies are assumed to range from 0.1 Mev to greater than 100 Mev. Using a number of computer models (AE-8, AP-8, SPE, ORBIT, SHIELDOSE), NASA has calculated the proper shielding thickness, 103.8 mils of Aluminum. These values can be used to determine the anticipated ambient radiation environment for the optical crossbar switch. Based upon a 7.5 year mission, the following radiation specifications are applicable:

(1) total radiation dose of 65 krads,

(2) single event upset rate (SEU) less than 10^{-9} errors/bit/day, even with burst levels of 10^{7} rad (Si)/second, and

(3) no latchup with 10^{8} rad/second.

The total radiation dose is the amount of radiation absorbed by the device over the complete duration of the mission. Single event upset and latchup are terms that apply primarily to electronic devices. An example of a single event upset is when a Dynamic Ram (DRAM) is struck by a cosmic ray and changes its logic state. An example of latchup is when a silicon controlled rectifier is exposed to radiation, becomes inoperable, and eventually burns out due to excess current draw.

4.2 Radiation Hardness of GaAs Electronic Devices

GaAs intrinsically has a high electron mobility, thus most integrated circuits with data rates exceeding a few hundred megabits per second must be fabricated using GaAs processes. In addition, most laser diodes and other high performance semiconductor light sources are based on GaAs fabrication technology because these materials have the correct bandgap necessary to emit light in the 800 - 1550 nm spectral range. Fortunately, GaAs integrated circuits are also inherently more radiation hard than hardened silicon IC technologies [8]. The main reason for this is that GaAs devices have no insulator or oxide between the gate and channel (as in Si MOSFET devices) which may collect an electrostatic charge in the presence of ionizing radiation. In addition, GaAs devices are very unlikely to form surface channels at GaAs-insulator interfaces, thus there is no problem with charging at these sites. The effect of the charge on MOS and other Si devices is to alter the device thresholds, and to eventually cause device failure.

GaAs devices have been found to tolerate gamma doses of 100 Mrad with pinchoff voltage shifts of less than 50 mv, many orders of magnitude better than Si MOS. With proper circuit design, GaAs IC devices are radiation hard to the following levels [8]:

Total Dose: > 10^7 rads (10^8 typical)

Transient Dose Rate: (upset): 10^8 rads/s (10^9 typical)

Transient Dose Rate: (survival): 10^{11} rads/s

GaAs electronics will be necessary in the optical transmitters and receivers for either the all-optical passive crossbar or electronic crossbar. From the information given above, we see that GaAs electronics easily meet the POP requirements and thus should be easily space-qualifiable. Some Si circuitry can also be used if properly shielded and packaged as described in [10]. Si electronics are adequate for the low speed switch controller in either the all-optical or electronic crossbar. Based on long-standing industry experience with design, manufacture and packaging of radiation-hard Si electronics, we again see no problems with space qualification of properly designed and packaged Si control modules.

4.3 Radiation Hardness of Optical Fiber

The most comprehensive series of tests on the radiation hardness of optical fibers themselves have been made by the Naval Research Laboratory.[5-7]. In addition, a detailed discussion of the various types of tests and manufacturer's literature from some fiber vendors (Corning) is available. This information is fairly extensive and is included in the SBIR Phase I final report [1].

The two most important factors are:

(1) the total dosage of radiation absorbed, and

(2) the rate at which the radiation is absorbed.

The major effect of radiation on fibers is a darkening (attenuation) proportional to the total dose (although some types of fiber have a saturation, in which the attenuation does not increase beyond some threshold). A second observation is that the attenuation of irradiated fibers generally decreases with time after exposure due to molecular rearrangement . This effect is called recovery or "healing". It is also found that darkening is slightly less severe at longer wavelengths, that darkening is more severe (by as much as an order of magnitude) at low temperatures (-55^o C) than at high temperatures (100^o C), and that darkening is more severe for highly doped-core fibers (graded-index and single mode) than for pure silica fibers. The following table gives some examples extracted from the extensive data in the references [5-7].

Table 4-1. Radiation darkening (dB/km) of optical fibers

Fiber type	Dose (rads) at 850 nm				Dose (rads) at 1300 nm			
	10^2	10^3	10^4	10^5	10^2	10^3	10^4	10^5
ITT single-mode	2	20	150	1500	NA			
Corning IVD single-mode	NA				0.2	2.0	20	220
Corning OVD single-mode	NA				0.2	0.8	8.0	22

Note that even at a total dose of 10^5 rads, a dose greater than the 65 krad maximum expected for POP structure modules, a fiber such as Corning OVD has a maximum attenuation of 22 dB/km. In the CHRPS system, the maximum interconnection distance is much less than 0.1 km, so that even under these radiation conditions the additional induced attenuation would be less than 2.2 dB. These results also do not include recovery with time, an effect that would also improve these estimates.

A final observation is that radiation effects are not linear over a wide range; it is incorrect to extrapolate to different doses or dose-rates; also the radiation-induced attenuation varies widely from fiber to fiber depending on doping, impurity concentration, and manufacturing techniques. The radiation hardness of some types of fiber can be improved "burn in," i.e., pre-exposing them to radiation before installation.

From this, we conclude that typical optical fibers to be used in CHRPS should be able to withstand the POP radiation environment. Many improvements can be made by specially selecting the type of fiber and special shielding of critically exposed parts. These tasks are normally done as part of any spacecraft engineering and qualification procedure.

In summary, the primary effect of radiation on optical fiber is an increase in attenuation. Sometimes this effect is temporary, while other times it is permanent. The amount of attenuation and the recovery time vary from fiber to fiber. Pure silica core fiber operating in the 1.3 μm window appears to have the best performance. It appears that radiation-hardened fiber with an attenuation of approximately 20 dB/km can be obtained from Corning. Thus, the radiation effects in fiber should not be a major driver on the design of a space-qualified optical crossbar switch, since the maximum fiber length in such a system is estimated to be 100 m.

4.4 Radiation Experiments on PDLC Arrays and GRIN Lenses

Experiments were designed to expose the PDLC array, its components, and GRIN lenses to a radiation environment similar to that expected on the EOS platform and to determine if any significant degradation occurs in the operation of these devices. Separate experiments were carried out for the following two types of radiation:

(1) 1 Mev electrons, and

(2) 10 Mev protons.

4.4.1 Electron Radiation Experiments

The electron radiation experiments were carried out by Dr. Carlos Vargas-Aburto of Kent State at NIST during the week of 26 August, 1991. For each radiation dose level, 1 Mev electrons were used to simultaneously bombard four adjacent elements of the PDLC array, a sample of the bare polyester substrate used in the array, a sample of the ITO-coated substrate, and two GRIN lenses. Irradiation was made at equally spaced dose levels, starting at a nominal value of 10 krads, with increments of 10 krads up to and including a maximum dose of 70 krads,

A Van de Graaf accelerator was used to carry out the irradiations. The irradiations were performed in air at room temperature. Calibration of the accelerator in terms of dose was performed first. This required the use of a special type of radiochromic film whose coloration changes in a reproducible way when exposed to different electron doses. Primary calibration of the films was made at NIST using a beta source of known activity.

Special precautions were taken to assure satisfactory uniformity of the beam over distances corresponding to the dimensions of the custom-built sample holder. A beam with a uniformity of better than 10% over a distance of about 12 cms was obtained.

Visual observations after the irradiations indicated no discernible signs of damage for the PDLC arrays or the polyester films, with or without ITO coating. Measurements were made at Optivision of the insertion loss and extinction ratio of the PDLC array after irradiation. Averaging was done over the sets of four PDLC array elements which were subjected to the same radiation dose level. Figures 4-1 and 4-2 show the excess PDLC insertion loss and extinction ratio, respectively, as a function of electron radiation dose level. The values are referenced to the average insertion loss of cells which were not irradiated. These figures indicate that no significant damage to the static optical characteristics of the PDLC array has occurred due to electron irradiation.

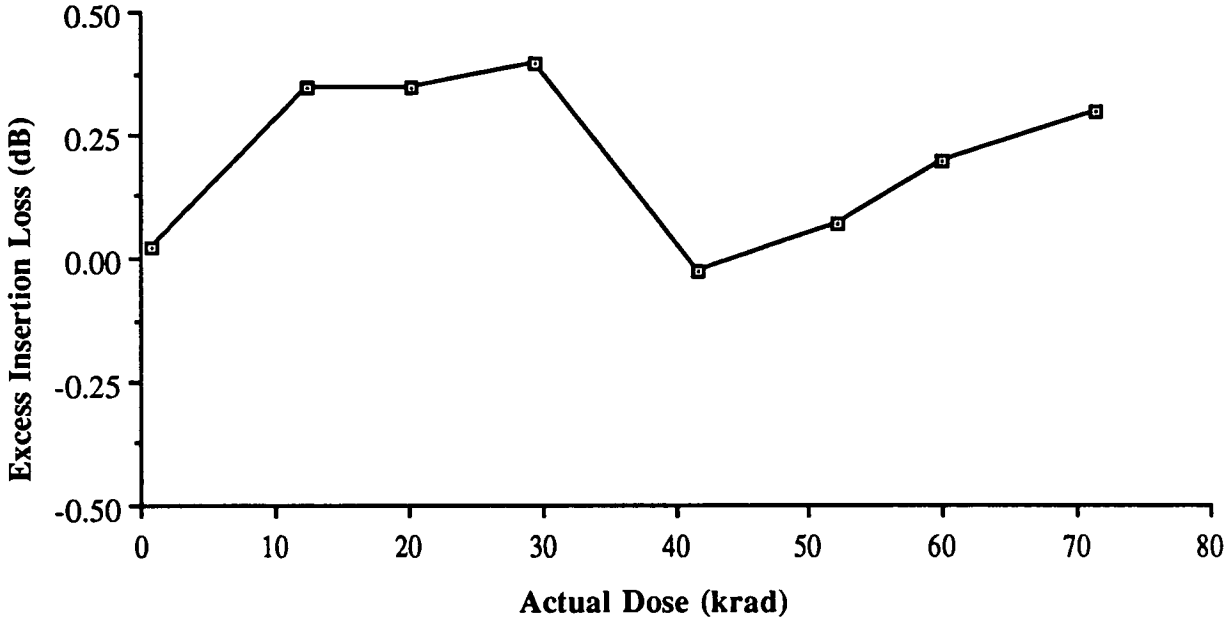

Figure 4-1. Excess insertion loss of electron-irradiated PDLC array.

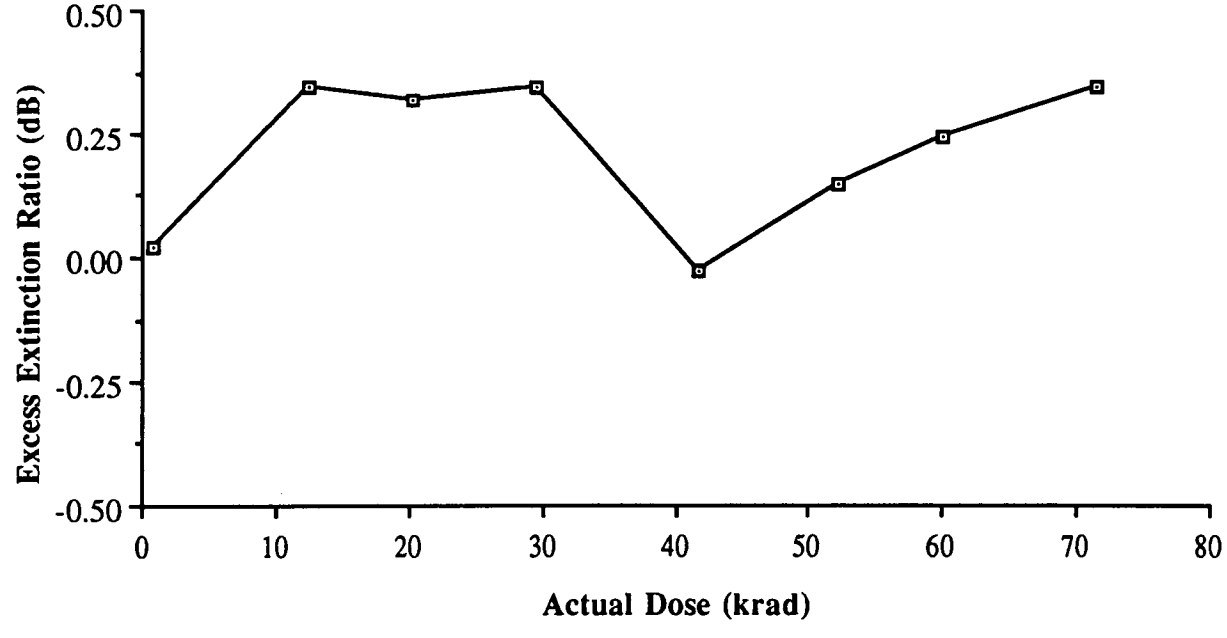

Figure 4-2. Excess extinction ratio of electron-irradiated PDLC array.

Measurements were also made at Optivision of the insertion loss of the GRIN lenses after irradiation. Figure 4-3 shows the GRIN lens excess insertion loss, averaged over the two lenses subjected to the same dose level, as a function of radiation dose level. Clearly, the GRIN lenses are effected by the radiation. The excess insertion loss due to the maximum dose level is approximately 1 dB. Since there are two GRIN lenses in each signal path, an additional 2 dB of optical loss must be accommodated in the optical power budget due to electron irradiation of the GRIN lenses. This degradation is well within the 12 dB excess power margin of the optical crossbar system.

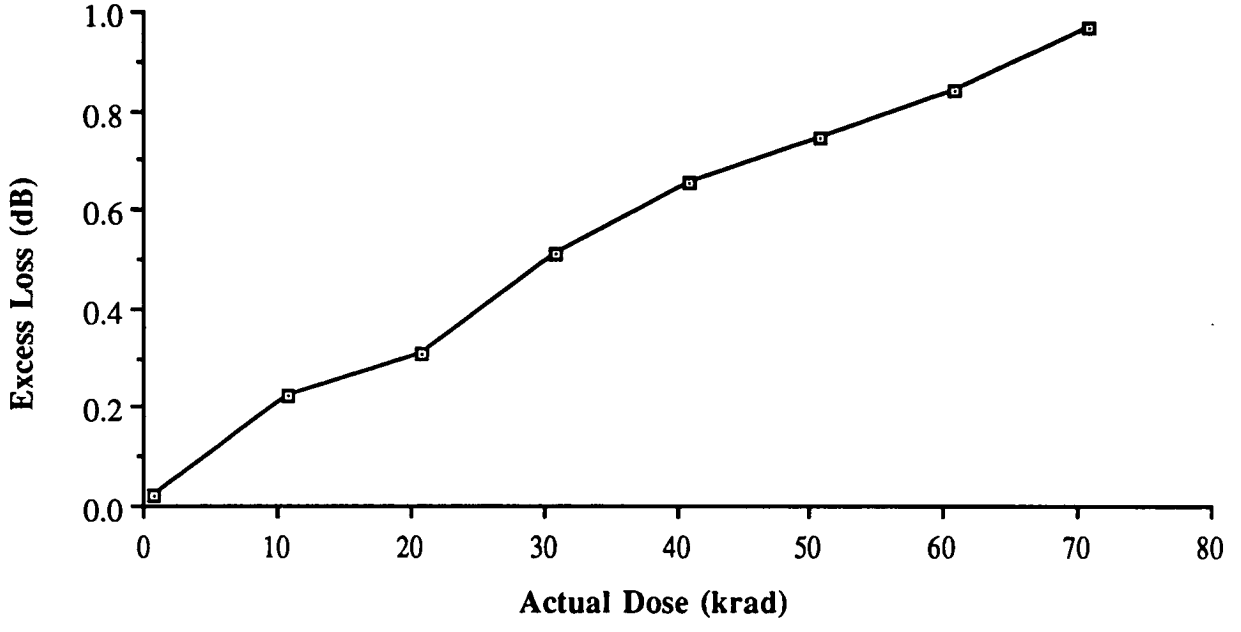

Figure 4-3. Excess insertion loss of electron-irradiated GRIN lenses.

4.4.2 Proton Radiation Experiments

A similar proton irradiation experiment was carried out by Dr. Vargas-Aburto at Western Michigan University at Kalamazoo, MI during the week of 14 October 1991. A proton Van de Graaf accelerator was used as the radiation source. Due to the size of the proton beam, it was necessary to irradiate the PDLC array, the PDLC substrates and the pairs of GRIN lenses on separate runs. As a result, the actual absorbed dose levels varied slightly between the different elements tested. In addition, only 3 adjacent PDLC cells were irradiated at the same nominal dose level. This was again due to the fact that the proton beam was not large enough to provide a uniform illumination of the four cells.

Measurements were made at Optivision of the insertion loss and extinction ratio of the PDLC array and insertion loss of the GRIN lenses. Averages were taken over the corresponding number of illuminated elements. Figures 4-4 and 4-5 show the excess PDLC insertion loss and extinction ratio of the PDLC array, respectively, as a function of the proton radiation dose level. The values are referenced to the average insertion loss of cells which were not irradiated. Again, these figures indicate no significant damage to the static optical characteristics of the PDLC array due to proton irradiation. The small variations shown are essentially random, corresponding to the variations in the individual cells within the PDLC array.

Figure 4-6 shows the GRIN lens excess insertion loss, averaged over the two lenses subjected to the same dose level, as a function of radiation dose level. Very little excess insertion loss is evident due to the fact that the 10 Mev protons were of such high energy that they passed through the samples with little effect.

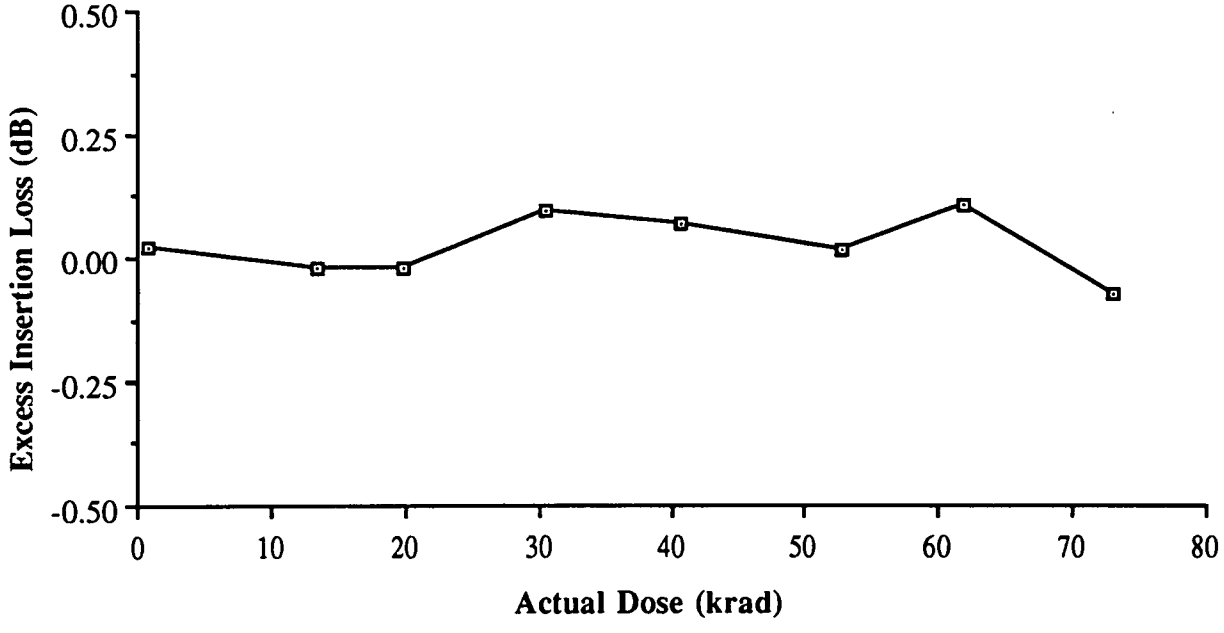

Figure 4-4. Excess insertion loss of proton-irradiated PDLC array.

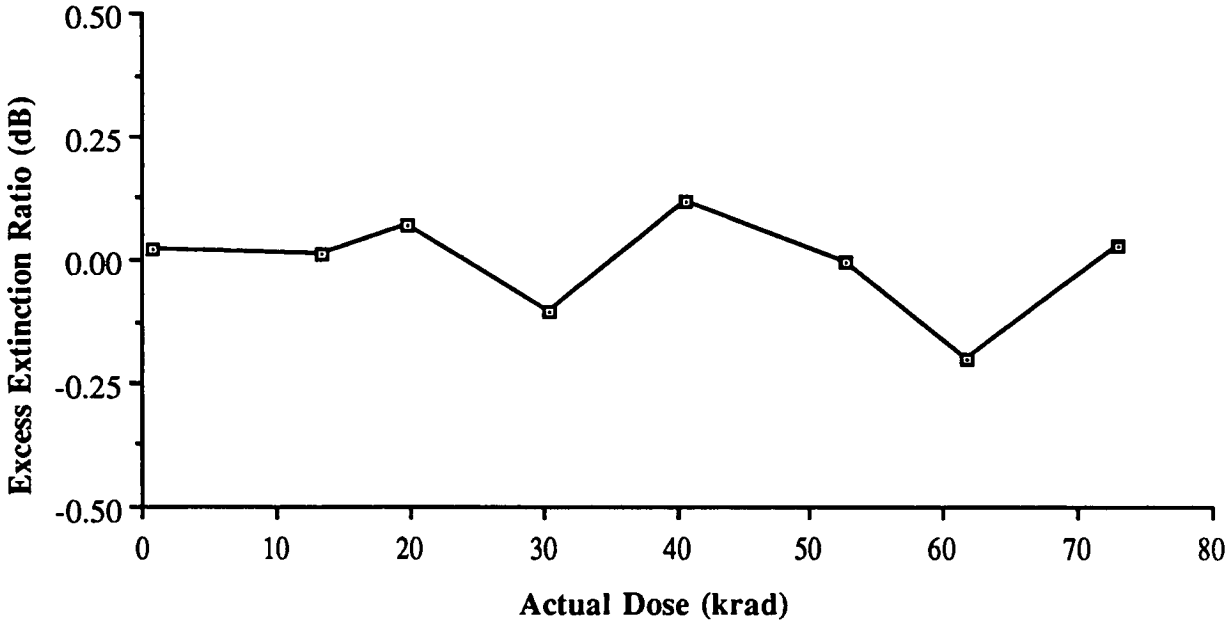

Figure 4-5. Excess extinction ratio of proton-irradiated PDLC array.

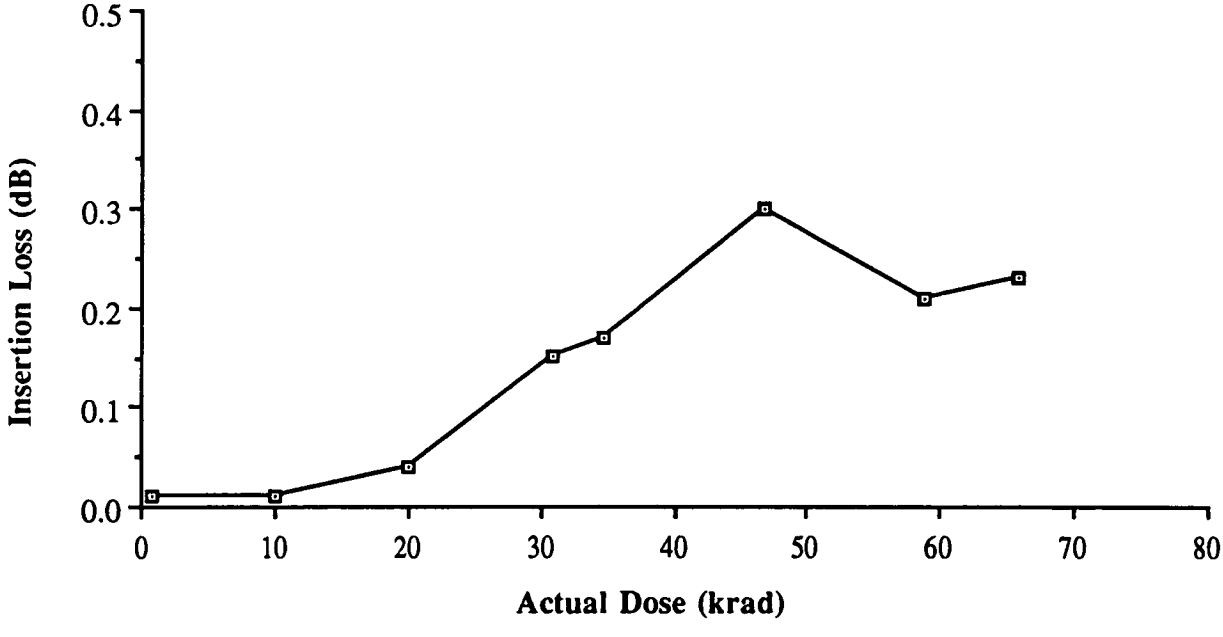

Figure 4-6. Excess insertion loss of proton-irradiated GRIN lenses.

5. Conclusions and Recommendations

5.1 Conclusions

All of the goals of this Phase II program have been successfully achieved. The overall conclusion is that a general purpose all-optical (data path) switch has been successfully demonstrated as part of a ground-based simulation of an onboard spacecraft high speed data network.

An 8x8 all-optical crossbar switch based on a matrix-vector multiplier design and appropriate interfaces was delivered to NASA Goddard and used in a demonstration of a CHRPS optical switching network. The optical crossbar itself uses polymer dispersed liquid crystal (PDLC) shutters, resulting in lower power requirements, simplified drive electronics, lower insertion loss, and freedom from polarization sensitivity.

Some initial radiation testing of the optical components and shutters in the crossbar switch was performed. The liquid crystal shutter assemblies, polyester films with and without conductive indium-tin-oxide (ITO) coatings, and gradient-index (GRIN) lenses were irradiated using both 1 Mev electrons and 10 Mev protons. The results are that there was no significant change to the optical characteristics of the shutter assemblies, or their components, after irradiation. The only noticeable change was a slight increase of the excess loss of the GRIN lenses subjected to electron radiation (essentially a linear increase in excess loss from 0 dB to 1.0 dB as the radiation dose increased from 0 to 70 krad). This increase in excess loss is well within the available power margins of the optical transmitters and receivers used in the network.

These initial experiments have shown no fundamental reasons why optical crossbar switch systems cannot tolerate the radiation environment of a polar orbit. Obviously, there is a great deal of additional work needed to confirm the initial results of our tests, and extensive testing of all components, including polarizers, liquid crystal materials, polymer substrates, interface and crossbar drive electronics, fibers, fiber-optic transmitters and receivers is needed. With care taken to use appropriate packaging and shielding techniques, the selected use of GaAs circuitry in critical areas, and a careful selection of fibers that are radiation-resistant, all-optical crossbar network switching systems should meet the POP radiation requirements and thus should be space-qualifiable.

Additional factors for space qualification are temperature and environmental stability, mechanical robustness and rigidity, and vibration resistance. We feel that fiber-optic systems, including transmitters, receivers, and passive switches having spatial light modulator arrays with liquid crystals, have no moving parts and thus can be engineered and packaged to withstand the same specifications as electronic systems for space.

5.2 Recommendations

The overall recommendation is that NASA continue to support optical switching and high speed data networks because of:

(1) the many application requirements and mission needs which this technology can support, and

(2) the rapidly evolving technology base in optical switching which will result in significant improvements when compared to electronic switching.

Requirements for high data rate optical networks include spacecraft, airborne and ground based applications. Spacecraft applications include systems such as CHRPS which interconnect sensors, processors, data links and possibly displays for manned spacecraft. Switching of high data rate communication crosslinks is an additional spacecraft application. Airborne applications include high speed optical networks and data busses for advanced avionics architectures. In many cases, these applications have been motivated by the introduction of fiber optic links to save space, weight, size, and reduce EMP, EMI, and RF interference. Optical switching then becomes advantageous for increasing data rates, and for elimination of additional electronic-to-optical and optical-to-electronic conversion. Ground applications of optical switching include switching of antenna feeds, for example, from space tracking networks and high speed local area networks such as those supported by the HPCC and NREN programs.

The recommendation is that NASA continue to support optical switching to fully realize its potential for the above cited applications. Development programs are need in four principal areas:

(1) active switch technology,

(2) compatibility with existing lightwave protocols,

(3) integration and packaging, and

(4) space qualification testing.

Active switch technology needs to be developed in order to realize larger switch sizes (to overcome inherent splitting and combining losses) and for some applications to improve the switching speed and latency involved in setting up the switch connections. Passive switches, such as those demonstrated in this program, will generally be limited to 8x8 or 16x16 in size. Active switches with the proper implementation of distributed gain [12] are almost unlimited in size. Also, many applications such as high speed avionics data networks will require faster switching than can be achieved with the passive shutter technology demonstrated in this program. This includes both the

time to compute the desired state of the switch as well as the time to physically change the shutter. With active switching elements, depending on the control scheme and the distances involved, reconfiguration times on the order of 10 microseconds are achievable.

Optical switches can and should be developed which are compatible with existing lightwave protocols and standards. Although the application for self-contained networks such as CHRPS may not require interoperability or connectivity with other networks, emerging lightwave protocols such as HIPPI, Fiber Channel, and SONET will motivate the development and availability of hardware components such as clock recovery chips and parallel to serial converters. Also, it is unlikely that major applications such as the Space Station would take the risk of implementing non-standard network protocols. Thus the development of optical switches which are compatible with standard protocols, and can in many cases retrofit electronic switches using these protocols, is desirable.

Integration and packaging will require substantial development in order for optical switches to realize their potential, particularly for spacecraft and airborne applications. The size of the optics module for the switch developed under this contract could be reduced by orders of magnitude by integrating the shutter and splitter/combiner functions onto one integrated chip. Development efforts have been initiated [13] and should be pursued to achieve NASA's goals of reduced weight, size and power. Active optical crossbar chips can be developed and used as modules for both achieving larger switch sizes as well as reducing the size, weight and power of the switch. When combined with an integrated electronic controller, the reduction in size and weight of the optical switch could be substantial. In addition these improvements would result in a significant reduction in cost as well as increasing the reliability of the switch.

The final recommendation is that NASA, perhaps in cooperation with the DoD, pursue a program to space qualify optical switches, particularly in terms of radiation testing. The use of optical switches on a major NASA or DoD mission without prior flight testing would clearly incur a large risk. It is recommended, therefore, that an optical switch package be developed and space test bed which would include different switch technology elements such as spatial light modulators, splitters, combiners, transmitters, receivers, and other optical switching components .

6. References

[1] Optivision, Inc., Final Report, NASA/GSFC Phase I SBIR Contract NAS5-30501, "Fiber Optic Interconnection Networks for Spacecraft," July 1989.

[2] A.R. Dias, R.F. Kalman, J.W. Goodman and A.A. Sawchuk, "Fiber-optic Crossbar Switch with Broadcast Capability," *Optical Engineering*, vol. 27, no. 11, pp. 955-960, November 1988.

[3] E.G. Stassinopoulos and J.P. Raymond, "The Space Radiation Environment for Electronics," *Proceedings of the IEEE*, vol. 76, no. 11, November 1988.

[4] J.D. Weiss, "The Radiation Response of a Selfoc Microlens," *Journal of Lightwave Technology*, vol. 8, no. 7, July 1990.

[5] E.J. Friebele, K.J. Long and M.E. Gingerich, "Radiation Damage in Single Mode Optical Fiber Waveguides," *Proc. Fifth Topical Meeting on Optical Fiber Communications and Conference on Lasers and Electro-Optics*, Optical Society of America, 1982.

[6] W.B. Beck, T.L. Reinhardt and B. Skutnik, "Radiation-hardened Fibers: Asking the Right Questions," *Photonics Spectra,* May 1986.

[7] E.J. Friebele, C.A. Askins, K.J. Long and M.E. Gingerich, "Temperature and Dose Rate Dependence of Radiation Damage in Single Mode and Multimode Optical Fiber Waveguides," *Proc. Fifth Topical Meeting on Optical Fiber Communications and Conference on Lasers and Electro-Optics*, Optical Society of America, 1982.

[8] GigaBit Logic, Inc., *GaAs IC Data Book and Designer's Guide*, GigaBit Logic, Inc., Newbury Park, CA 91320, May 1988.

[9] Dr. Carlos Vargas-Aburto, Kent State University (private communication).

[10] J. Schaefer, NASA Space Station Freedom Design Note SSP-DN-ENV-014A, "Radiation Tolerance Design Criterion," GE Astro-Space Division, 6 July 1989.

[11] C. Sekhar, NASA Space Station Freedom Design Note NASA SSP-DN-ENV-017, "Radiation Environment of EOS Platform for 705 km Altitude at 98.2 Degree Inclination," GE Astro-Space Division, 16 April 1990.

[12] R.F. Kalman, L.G. Kazovsky, and J.W. Goodman, "Space Division Switches Based on Semiconductor Optical Amplifiers," to be published in *Photonics Technology Letters.*

[13] Optivision, Inc., Technical Proposal to U.S. Air Force Wright Laboratory, PRDA 92-19-AAK, "Very High Speed Optical Network (VHSON)," May 1992.

NASA
National Aeronautics and Space Administration

Report Documentation Page

1. Report No.	2. Government Accession No.	3. Recipient's Catalog No.

4. Title and Subtitle
Fiber-Optic Interconnection Networks for Spacecraft

5. Report Date
May 1992

6. Performing Organization Code

7. Author(s)
Robert S. Powers, Kelvin K. Chau, Alexander A. Sawchuk and Larry R. McAdams

8. Performing Organization Report No.

10. Work Unit No.

9. Performing Organization Name and Address
Optivision, Inc.
4009 Miranda Avenue
Palo Alto, CA 94304

11. Contract or Grant No.
NAS5-30896

13. Type of Report and Period Covered
Final Report
May 22, 1990 - May 21, 1992

12. Sponsoring Agency Name and Address
NASA Goddard Space Flight Center
Greenbelt Road
Greenbelt, MD 20771

14. Sponsoring Agency Code
Code 735

15. Supplementary Notes

16. Abstract

The overall goal of this effort was to perform the detailed design, development and construction of a prototype 8x8 all-optical fiber-optic crossbar switch. The switch was to use low-power liquid crystal shutters capable of operation in a network with suitable fiber-optic transmitters and receivers at a data rate of 1 Gb/s and wavelength of 1300 nm. An 8x8 matrix vector multiplier (MVM) architecture optical crossbar switch was constructed. Polymer dispersed liquid crystal (PDLC) shutters were used because of their low power requirements, simple drive electronics, lack of polarization sensitivity, and small insertion loss. The delivered switch was integrated successfully into the Configurable High Rate Processing System (CHRPS) Initial Test Bed, which is a ground-based fiber-optic network test bed system whose intent is to demonstrate the feasibility of high bandwidth data communication in a spacecraft environment..

The delivered crossbar switch had significantly improved performance compared to previous optical crossbar switches in terms of lower insertion loss, improved loss uniformity, reduced size, and reduced power consumption. An average insertion loss of 14.8 dB was obtained, with a total variation of 2.3 dB across all combinations of input and output ports. The average optical extinction ratio for the switch was 18.5 dB, while typical shutter turn-on and turn-off times were 10 and 30-40 msec, respectively, suitable for the particular NASA application. The prototype switch had a volume of 1.34 cu.ft., weighed less than 30 pounds and consumed 34 watts.

Additional work is recommended in the areas of: (1) active switch technology, for larger switch sizes (number of nodes) and improved switching speed, (2) compatibility with lightwave protocols, to take advantage of hardware component availability, (3) integration and packaging, for reduction in size, weight and power, and (4) space qualification testing.

17. Key Words (Suggested by Author(s))	18. Distribution Statement
fiber optics optical interconnections optical crossbar switch photonic switching signal distribution liquid crystals	

19. Security Classif. (of this report)	20. Security Classif. (of this page)	21. No. of Pages	22. Price
Unclassified	Unclassified	42	

NASA Form 1626